Impact of dust enrichment on Mediterranean plankton communities under present and future conditions of pH and temperature: an experimental overview

Frédéric Gazeau[1], Céline Ridame[2], France Van Wambeke[3], Samir Alliouane[1], Christian Stolpe[1], Jean-Olivier Irisson[1], Sophie Marro[1], Jean-Michel Grisoni[4], Guillaume De Liège[4], Sandra Nunige[3], Kahina Djaoudi[3], Elvira Pulido-Villena[3], Julie Dinasquet[5,6], Ingrid Obernosterer[6], Philippe Catala[6], Cécile Guieu[1]

[1] Sorbonne Université, CNRS, Laboratoire d'Océanographie de Villefranche, LOV, 06230 Villefranche-sur-Mer, France

[2] CNRS-INSU/IRD/MNHN/UPMC, LOCEAN: Laboratoire d'Océanographie et du Climat: Expérimentation et Approches Numériques, UMR 7159, 75252 Paris Cedex 05, France

[3] Aix-Marseille Université, Université de Toulon, CNRS/INSU, IRD, MIO, UM 110, 13288, Marseille, France

[4] Sorbonne Université, CNRS, Institut de la Mer de Villefranche, IMEV, 06230 Villefranche-sur-Mer, France

[5] Scripps Institution of Oceanography, University of California San Diego, USA

[6] CNRS, Sorbonne Université, Laboratoire d'Océanographie Microbienne, LOMIC, F-66650 Banyuls-sur-Mer, France

Correspondence to: Frédéric Gazeau (f.gazeau@obs-vlfr.fr)

Keywords: Mediterranean Sea; Atmospheric deposition; Plankton community ; Ocean acidification; Ocean warming

Abstract

In Low Nutrient Low Chlorophyll areas, such as the Mediterranean Sea, atmospheric fluxes represent a considerable external source of nutrients likely supporting primary production especially during stratification periods. These areas are expected to expand in the future due to lower nutrient supply from sub-surface waters caused by enhanced stratification, likely further increasing the role of atmospheric deposition as a source of new nutrients to surface waters. Yet, whether plankton communities will react differently to dust deposition in a warmer and acidified environment remains an open question. The impact of dust deposition both in present and future climate conditions was assessed through three perturbation experiments in the open Mediterranean Sea. Climate reactors (300 L) were filled with surface water collected in the Tyrrhenian Sea, Ionian Sea and in the Algerian basin during a cruise conducted in May/June 2017 in the frame of the PEACETIME project. The experimental protocol comprised two unmodified control tanks, two tanks enriched with a Saharan dust analog and two tanks enriched with the dust analog and maintained under warmer (+3 ºC) and acidified (-0.3 pH unit) conditions. Samples for the analysis of an extensive number of biogeochemical parameters and processes were taken over the duration of the experiments (3-4 d). Here, we present the general setup of the experiments and the impacts of dust seeding and/or future climate change scenario on nutrients and biological stocks. Dust addition led to a rapid and maximum input of nitrate whereas phosphate release from the dust analog was much smaller. Our results showed that the impacts of Saharan dust deposition in three different basins of the open Northwestern Mediterranean Sea are at least as strong as those observed previously in coastal waters. However, interestingly, the effects of dust deposition on biological stocks were highly different between the three investigated stations and could not be attributed to differences in their degree of oligotrophy but rather to the initial metabolic state of the community.

Finally, ocean acidification and warming did not drastically modify the composition of the autotrophic assemblage with all groups positively impacted by warming and acidification, suggesting an exacerbation of effects from atmospheric dust deposition in the future.

1. Introduction

Atmospheric deposition is well recognized as a significant source of micro- and macro-nutrients for surface waters of the global ocean (Duce et al., 1991; Jickells et al., 2005; Moore et al., 2013). The potential modulation of the biological carbon pump efficiency and the associated export of carbon by atmospheric deposition events are still poorly understood and quantified (Law et al., 2013). This is especially true for Low Nutrient Low Chlorophyll (LNLC) areas where atmospheric fluxes can play a considerable role in nutrient cycling and that represent 60% of the global ocean surface area (Longhurst et al., 1995) as well as 50% of global carbon export (Emerson et al., 1997). These regions are characterized by a low availability of macronutrients (N, P) and/or metal micronutrients (e.g. Fe) that can severely limit or co-limit phytoplankton growth during large periods of year. The Mediterranean Sea is a perfect example of these LNLC regions and exhibits chlorophyll *a* concentrations of less than 0.2 μg L^{-1} all year round over most of its area, except in the Ligurian Sea where relatively large blooms can be observed in late winter-early spring (e.g. Mayot et al., 2016). Recent assessments showed that the atmospheric input of nutrients in the Mediterranean Sea is of the same order of magnitude as riverine inputs (Powley et al., 2017), making the atmosphere a considerable external source of nutrients (Richon et al., 2018). Atmospheric depositions are mostly in the form of pulsed inputs of aerosols from both natural (Saharan dust) and anthropogenic origins (e.g. Bergametti et al., 1989; Desboeufs et al., 2018). Dust deposition is mainly associated with wet deposition and occurs in the form of extreme events (Loÿe-Pilot and Martin, 1996). Ternon et al. (2010) reported on an average annual dust flux over four years of 11.4 g m^{-2} yr^{-1} (average during the period 2003–2007) at the DYFAMED station in the Northwestern Mediterranean Sea. In this region, the most important events reported in the 2010 decade amounted to ~22 g m^{-2} (Bonnet and Guieu, 2006; Guieu et al., 2010b). Atmospheric

deposition provides new nutrients to the surface waters (Guieu et al., 2010b; Kouvarakis et al., 2001; Markaki et al., 2003; Ridame and Guieu, 2002), Fe (Bonnet and Guieu, 2006) and other trace metals (Desboeufs et al., 2018; Guieu et al., 2010b; Theodosi et al., 2010), that represent significant inputs likely supporting the primary production especially during the stratification period (Ridame and Guieu 2002, Bonnet et al. 2005), although no clear correlation between dust and ocean color could be evidenced from long series of satellite observation (Guieu and Ridame, 2020).

Experimental approaches have shown that wet dust deposition events in the Northwestern Mediterranean Sea (the dominant deposition mode in that basin) present a highest positive impact, by supplying bioavailable new nutrients, compared to dry deposition on all tested parameters and processes (Guieu et al., 2014a), except for N_2 fixation (Ridame et al., 2014). This so-called fertilizing effect has been experimentally shown using microcosms or mesocosms where the wet deposition of Saharan dust analog strongly stimulated primary production and phytoplankton biomass (Guieu et al., 2014a; Ridame et al., 2014) but also modified the phytoplankton diversity (Giovagnetti et al., 2013; Lekunberri et al., 2010; Romero et al., 2011). However, besides phytoplankton, dust deposition modified also the bacterial community assemblage and led to even stronger enhancements of production and/or respiration rates (Pulido-Villena et al., 2014). The budgets established from four artificial seeding experiments during the DUNE project (Guieu et al., 2014a) showed that by stimulating predominantly heterotrophic bacteria, atmospheric dust deposition can enhance the heterotrophic behavior of these oligotrophic waters. This has the potential to reduce the fraction of organic carbon that can be exported to deep waters during the winter mixing period (Pulido-Villena et al., 2008) and ultimately limit net atmospheric CO_2 drawdown.

Another effect induced by Saharan dust deposition is the export of particulate organic carbon (POC) as lithogenic particles can aggregate and ballast dissolved organic matter (Bressac et

al., 2014; Desboeufs et al., 2014; Louis et al., 2017a; Ternon et al., 2010). This so-called lithogenic carbon pump can represent a major part of the carbon export following a dust deposition event (up to 50% during the DUNE experiment; Bressac et al., 2014). Recently, Louis et al. (2017a) showed that Saharan dust deposition triggers the abiotic formation of transparent exopolymeric particles (TEP), leading to the formation of organic-mineral aggregates, a formation process that is highly dependent on the quality and quantity of TEP-precursors initially present in seawater.

In response to ocean warming and increased stratification, open ocean nutrient cycles are being and will be perturbed in the next decades with a high confidence of having regionally variable impacts on primary producers (IPCC, 2019). Overall, LNLC areas are expected to expand in the future (Irwin and Oliver, 2009; Polovina et al., 2008) due to lower nutrient supply from sub-surface waters (Behrenfeld et al., 2006), likely further increasing the role of atmospheric deposition as a significant source of new nutrients to surface waters. The ongoing warming and acidification of the global ocean (IPCC, 2019), both also evidenced in the Mediterranean Sea (e.g. Kapsenberg et al., 2017; The Mermex group, 2011) raise the question on whether plankton communities will react differently to dust deposition in a warmer and acidified environment. Although dependent on resource availability, it is well known that remineralisation by bacteria is subject to positive temperature control (López-Urrutia and Morán, 2007). Under severe nutrient limitation, there is no evidence that warming will lead to an enhancement of primary productivity (Marañón et al., 2018), further pushing the balance towards net heterotrophy in oligotrophic areas.

With respect to ocean acidification, an *in situ* mesocosm experiment conducted during the summer stratified period in the Northwestern Mediterranean Sea showed that the plankton community was rather insensitive to this perturbation under strong nutrient limitation (Maugendre et al., 2017, and references therein). This is coherent with results from Maugendre et al. (2015), based on a batch experiment, showing that, under nutrient-depleted conditions in late winter, ocean

119 acidification has a very limited impact on the plankton community and that small species (e.g.
120 Cyanobacteria) might benefit from warming with a potential decrease of the export and energy
121 transfer to higher trophic levels. In contrast, in more eutrophic coastal conditions, Sala et al. (2016)
122 showed that ocean acidification exerted a positive effect on phytoplankton, especially on pico- and
123 nano-phytoplankton. Similarly, Neale et al. (2014) showed in a coastal ecosystem of the Alboran
124 Sea that ocean acidification could lead, although moderately, to high chlorophyll levels under low
125 light conditions with an opposite effect under high irradiance.

126 To date and to the best of our knowledge, there has been no attempts to evaluate the
127 behavior of plankton communities after the deposition of atmospheric particles in the context of
128 future levels of temperature and pH. Yet, following the recommendation from Maugendre et al.
129 (2017), any perturbation experiment for future climate conditions in the Mediterranean Sea should
130 consider atmospheric deposition as a source of new nutrients and consider both temperature and pH
131 as external forcings. Such experiments were conducted in the frame of the PEACETIME project
132 (ProcEss studies at the Air-sEa Interface after dust deposition in the MEditerranean sea;
133 http://peacetime-project.org/) during the cruise on board the R/V “Pourquoi Pas?” in May/June
134 2017. The project aimed at extensively studying and parameterizing the chain of processes
135 occurring in the Mediterranean Sea after atmospheric deposition, especially of Saharan dust, and to
136 put them in perspective of on-going environmental changes (Guieu et al., 2020). During that cruise,
137 three perturbation experiments were conducted in climate reactors (300 L tanks) filled with surface
138 water collected in the Tyrrhenian Sea (TYR), Ionian Sea (ION) and in the Algerian basin (FAST;
139 Fig. 1). Six tanks were used to follow simultaneously and with a high temporal resolution, the
140 evolution of biological activity and stocks, nutrients stocks, dissolved organic matter as well as
141 particles dynamics and export, following a dust deposition event simulated at their surface, both
142 under present environmental conditions and following a realistic climate change scenario for 2100

(ca. +3 °C and -0.3 pH units; IPCC, 2013). In this manuscript, we will present the general setup of the experiments, the impacts of dust seeding and/or future climate change scenario on nutrients and biological stocks. Among several other manuscripts related to these experiments that are introduced here, a companion paper will be focusing on plankton metabolism (primary production, heterotrophic prokaryote production) as well as on carbon budget.

2. Material and Methods

2.1. General setup

Six experimental tanks (300 L; Fig. 2) in which the irradiance spectrum and intensity can be finely controlled and in which future ocean acidification and warming conditions can be fully reproduced were installed in a temperature-controlled container. The tanks are made of high-density polyethylene (HDPE) and were trace-metal free in order to avoid contaminations, with a height of 1.09 m, a diameter of 0.68 m, a surface area of 0.36 m^2 and a volume of 0.28 m^3. All tanks were cleaned before the experimental work following the protocol described by Bressac and Guieu (2013). A weak turbulence was generated by a rotating PVC blade (9 rpm) in order to mimic natural conditions. Each tank was equipped with a lid containing six rows of LEDs (Alpheus©). Each of these rows were composed of blue, green, cyan and white units in order to mimic the natural sun spectrum. At the conical base of each tank, a polyethylene (PE) bottle collecting the exported material from above was screwed onto a polyvinyl chloride (PVC) valve that remained open during the duration of the whole experiment. Photosynthetically active radiation (PAR; 400-700 nm) and temperature were continuously monitored in each tank using respectively QSL-2100 Scalar PAR Irradiance Sensors (Biospherical Instruments©) and pt1000 temperature sensors (Metrohm©) connected to a D230 datalogger (Consort©).

The experimental protocol comprised two unmodified control tanks (C1 and C2), two tanks enriched with Saharan dust (D1 and D2) and two tanks enriched with Saharan dust and maintained under warmer (+3 ºC) and acidified (-0.3 pH unit) conditions (G1 and G2). The atmosphere above tanks C1, C2, D1 and D2 was flushed with ambient air (ca. 400 ppm, 6 L min^{-1}) and tanks G1 and G2 were flushed with air enriched with CO_2 (ca. 1000 ppm, 6 L min^{-1}) in order to prevent CO_2

degassing from the acidified tanks. CO_2 partial pressure (pCO_2) in both ambient air and CO_2-enriched air was monitored using two gas analysers (LI-820, LICOR©). The CO_2 concentration in the CO_2-enriched air was manually controlled through small injections of pure CO_2 (Air Liquide©) using a mass flow controller.

Three experiments were performed at the long duration stations TYR, ION and FAST. The tanks were filled by means of a large peristaltic pump (Verder© VF40 with EPDM hose, flow of 1200 L h^{-1}) collecting seawater below the base of the boat (depth of ~ 5 m), used to supply continuously surface seawater to a series of instruments during the entire campaign. In order to homogeneously fill the tanks, the flow was divided into six HDPE pipes distributing the water simultaneously into the different tanks. Overall, the filling of the six tanks took ~2 h (including rinsing and initial sampling, see thereafter). At the three stations, tanks were always filled at the end of the day before the start of the experiments: TYR (17/05/2017), ION (25/05/2017) and FAST (02/06/2017). While filling the tanks, this surface seawater was sampled for the measurements of selected parameters (sampling time = t-12h, see Table 1). After filling the tanks, seawater was slowly warmed using 500 W heaters, controlled by temperature-regulation units (COREMA©), in G1 and G2 overnight to reach an offset of +3 °C. ^{13}C-bicarbonate was added to all tanks at 4:00 am (local time; Gazeau et al., in preparation, this issue) and G1 and G2 were acidified by addition of CO_2-saturated filtered (0.2 µm) seawater (~1.5 L in 300 L; collected when filling the tanks at each station) at 4:30 am to reach a pH offset of -0.3. Sampling for many parameters took place prior to dust seeding (sampling time = t0, see Table 1). Dust seeding was performed between 7:00 and 9:00 (local time) in tanks D1, D2, G1 and G2. The same dust analog was used and the same dust flux was simulated as for the DUNE 2009 experiments described in Desboeufs et al. (2014). Briefly, the fine fraction (< 20 µm) of Saharan soils collected in southern Tunisia, which is a major source of dust deposition over the northwestern Mediterranean basin, was used in the seeding experiments.

The particle size distribution showed that 99% of particles had a size smaller than 0.1 µm, and that particles were mostly made of quartz (40%), calcite (30%) and clay (25%; Desboeufs et al., 2014). This collected dust underwent an artificial chemical aging process by addition of nitric and sulfuric acid (HNO_3 and H_2SO_4, respectively) to mimic cloud processes during atmospheric transport of aerosol with anthropogenic acid gases (Guieu et al., 2010a, and references therein). To mimic a realistic wet flux event of 10 g m^{-2}, 3.6 g of this analog dust were quickly diluted into 2 L of ultrahigh-purity water (UHP water; 18.2 MΩ cm^{-1} resistivity), and sprayed at the surface of the tanks using an all-plastic garden sprayer (duration = 30 min). The N and P total contents in the dust were 1.36 ± 0.09% of N and 0.055 ± 0.003% of P (see Desboeufs et al., 2014, for a full description of dust chemical composition). The experimental protocol included the analysis of an extensive number of biogeochemical parameters and processes, not all shown and discussed in this paper, that are listed in Table 1. The experiment at stations TYR and ION lasted 72 h (3 days) whereas the last experiment at station FAST was extended to four days. Seawater sampling was conducted 1 h (t1h), 6 h (t6h), 12 h (t12h), 24 h (t24h), 48 h (t48h) and 72 h (t72h) (+ 96 h = t96h for station FAST) after dust addition. Acid-washed silicone tubes were used for transferring the water collected from the tanks to the different vials or containers. For some parameters (e.g. nutrients, dissolved organic carbon), sampled seawater was filtered online at the exit of the tanks on sterile membrane filter capsules (gravity filtration with Sartobran© 300; 0.2 µm).

2.2. Analytical methods

2.2.1. Carbonate chemistry

Seawater samples for pH measurements were stored in 300 mL glass bottles with a glass stopper, pending analysis on board (within 2 h). Samples were transferred to 30 mL quartz cells and

absorbances at 434, 578 and 730 nm were measured at 25 °C on an Cary60 UV-Spectrophotometer (Agilent©) before and after addition of 50 µL of purified meta-cresol purple provided by Robert H. Byrne (University of South Florida, USA) following the method described by Dickson et al. (2007). pH on the total scale (pH_T) was computed using the formula and constants of Liu et al. (2011). The accuracy of pH measurements was estimated to 0.007 pH units, using a TRIS buffer solution (salinity 35, provided by Andrew Dickson, Scripps university, USA).

Seawater samples for total alkalinity (A_T; 500 mL) measurements were filtered on GF/F membranes and analyzed onboard within one day. A_T was determined potentiometrically using a Metrohm© titrator (Titrando 888) and a glass electrode (Metrohm©, ecotrode plus) calibrated using first NBS buffers (pH 4.0 and pH 7.0, to check that the slope was Nernstian) and then using a TRIS buffer solution (salinity 35, provided by Andrew Dickson, Scripps university, USA). Triplicate titrations were performed on 50 mL sub-samples at 25 ºC and A_T was calculated as described by Dickson et al. (2007). Titrations of standard seawater provided by Andrew Dickson (Scripps university, USA; batch 151) yielded A_T values within 5 µmol kg^{-1} of the nominal value (standard deviation = 1.5 µmol kg^{-1}, n = 40).

All parameters of the carbonate chemistry were determined from pH_T, A_T, temperature, salinity, as well as phosphate and silicate concentrations using the R package seacarb[1]. Propagation of errors on computed parameters was performed using the new function "error" of this package, considering errors associated with the estimation of A_T, pH_T as well as errors on dissociation constants (Orr et al., 2018).

[1] Seacarb: seawater carbonate chemistry with R. Gattuso, J.-P., J. M. Epitalon, H. Lavigne, J. C. Orr, B. Gentili, M. Hagens, A. Hofmann, A. Proye, K. Soetaert and J. Rae, 2018. https://cran.r-project.org/package=seacarb

2.2.2. Nutrients

Seawater samples for dissolved nutrients were filtered online (<0.2 µm), collected in polyethylene bottles and immediately analyzed on board. Nitrate + nitrite (NO_x) and silicate ($Si(OH)_4$) measurements were conducted using a segmented flow analyzer (AAIII HR Seal Analytical©) according to Aminot and Kérouel (2007)with a limit of quantification of 0.05 µmol L^{-1} for NO_x and 0.08 µmol L^{-1} for $Si(OH)_4$. In addition, for t-12h samples, the analysis of NO_x was also performed by a spectrometric method in the visible at 540 nm, with a 1 m Liquid Waveguide Capillary Cell (LWCC). The limit of detection was ~10 nmol L^{-1} and the reproducibility was ~6%. Also from samples taken at t-12h, the measurement of ammonium concentrations was performed on board using a Fluorimeter TD-700 (Turner Designs©) according to Holmes et al. (1999). This fluorimetric method is based on the reaction of ammonia with orthophtaldialdehyde and sulfite and has a limit of quantification of 0.01 µmol L^{-1}. Dissolved inorganic phosphorus (DIP) concentrations were quantified using the Liquid Waveguide Capillary Cell (LWCC) method according to Pulido-Villena et al. (2010). The LWCC was 2.5 m long and the limit of detection was 1 nmol L^{-1}.

2.2.3. Pigments

A volume of 2.5 L of sampled seawater was filtered onto GF/F filters, immediately frozen in liquid nitrogen and stored at -80 ºC pending analysis at the SAPIGH analytical platform at the Institut de la Mer de Villefranche (IMEV, France). Filters were extracted at -20 ºC in 3 mL methanol (100%) containing an internal standard (vitamin E acetate, Sigma©), disrupted by sonication and clarified one hour later by vacuum filtration through GF/F filters. The extracts were rapidly analyzed (within 24 h) on a complete Agilent© Technologies 1200 series HPLC system. The pigments were separated and quantified as described in Ras et al. (2008).

2.2.4. Flow cytometry

For the enumeration of autotrophic prokaryotic and eukaryotic cells, heterotrophic prokaryotes and heterotrophic nanoflagellates (HNF) by flow cytometry, subsamples (4.5 mL) were fixed with glutaraldehyde grade I 25% (1% final concentration), and incubated for 30 min at 4 °C, then quick-frozen in liquid nitrogen and stored at -80 °C until analysis. Samples were thawed at room temperature. Counts were performed on a FACSCanto II flow cytometer (Becton Dickinson©) equipped with 3 air-cooled lasers: blue (argon 488 nm), red (633 nm) and violet (407 nm). The separation of different autotrophic populations was based on their scattering and fluorescence signals according to Marie et al. (2010). *Synechococcus* spp. was discriminated by its strong orange fluorescence (585 ± 21 nm), and pico- and nano-eukaryotes were discriminated by their scatter signals of red fluorescence (> 670 nm). For the enumeration of heterotrophic prokaryotes, cells were stained with SYBR Green I (Invitrogen – Molecular Probes) at 0.025% (vol / vol) final concentration for 15 min at room temperature in the dark. Stained prokaryotic cells were discriminated and enumerated according to their right-angle light scatter (SSC) and green fluorescence at 530/30 nm. In a plot of green versus red fluorescence, heterotrophic prokaryotes were distinguished from autotrophic prokaryotes. For the enumeration of HNF, staining was performed with SYBR Green I (Invitrogen—Molecular Probes) at 0.05% (v/v) final concentration for 15-30 min at room temperature in the dark (Christaki et al., 2011). Cells were discriminated and enumerated according to their SSC and green fluorescence at 530/30 nm. Fluorescent beads (1.002 µm; Polysciences Europe©) were systematically added to each analyzed sample as internal standard. The cell abundance was determined from the flow rate, which was calculated with TruCount beads (BD biosciences©). Biomasses of each group were estimated based on conversion equations and/or factors found in the literature (see section 2.3).

2.2.5. Micro-phytoplankton and -heterotrophs

At t-12h (i.e. seawater sampled during the filling of the tanks), a volume of 500 mL was sampled in glass vials and immediately preserved in a 5% acidic Lugol's solution pending analysis. At the Laboratoire d'Océanographie de Villefranche (LOV, France), 100 mL aliquots were transferred to sedimentation chambers (Utermohl) and counted under an inverted microscope at 200 to 400 magnifications.

2.2.6. Mesozooplankton

At the end of each experiment (t+72h for TYR and ION and t+96 h for FAST, after artificial dust seeding), the sediment traps were removed, closed and stored with formaldehyde 4% (see Gazeau et al., in preparation, this issue). The valve at the base of the tanks was then reopened to let the remaining water inside the tanks (TYR 165-180 L; ION = 172.5 L and FAST = 150 L) pass through a large PVC sieve (100 µm). The organisms retained on that mesh were gently removed from the sieve using a washing bottle filled with filtered seawater (0.2 µm), and transferred directly inside a 250 mL bottle. The bottle was filled with the sample (1/3 of the volume), and was completed with formaldehyde 4% . The zooplankton digital images were obtained using a ZooSCAN (Hydroptic©; Gorsky et al., 2010) at the PIQv-platform of EMBRC-France. The identification of species was performed by automatic comparison with the library data set EcoTaxa (https://ecotaxa.obs-vlfr.fr/, last access: 17/04/2020) and then all validated and corrected by a human operator.

2.3 Computations

The maximum percentage of dissolution from dust observed with respect to N and P was calculated considering that these evapo-condensated dust contain 1.36 ± 0.09% of N and 0.055 ± 0.003% of P (Desboeufs et al., 2014). Based on maximal concentrations observed in the D and G tanks after seeding (two discrete sampling within 6 h), one can estimate the maximal % of dissolution of dust in seawater during the three experiments:

$$\%_{dissolution} = \frac{CONC_{max} - CONC_{init}}{CONC_{dust}} . 100 \quad (1)$$

where $CONC_{init}$ is the concentration of the corresponding nutrient in each tank before seeding (t0), $CONC_{max}$ corresponds to the concentration of the corresponding nutrient in each tank when nutrient concentration was at a maximum over the first 6 h after seeding as observed based on our discrete sampling procedure, and $CONC_{dust}$ corresponds to the maximum input of each nutrient, if 100% of its total concentration in the dust analog dissolves (as estimated based on dust chemical composition; Desboeufs et al., 2014; see above).

As micro-phytoplankton counting was not performed throughout the experiment, as a first approximation, autotrophic biomass was calculated as the sum of carbon contained in *Synechococcus*, pico-eukaryotes and nano-eukaryotes (abundances based on flow cytometry) and is therefore restricted to the fraction < 20 µm. For *Synechococcus*, conversion to carbon units were done considering 250 fg C $cell^{-1}$ (Kana and Glibert, 1987), while the equation proposed by Verity et al. (1992; 0.433 $BV^{0.863}$ where BV refers to the biovolume) was used for pico- and nano-eukaryotes assuming a spherical shape and a diameter of 2 and 6 µm for the two groups, respectively. Percentages of these different groups were calculated in order to estimate the composition of the communities at the start and its evolution during the experiments. Furthermore, heterotrophic

biomass was computed as the sum of heterotrophic prokaryotes biomass and heterotrophic nanoflagellates biomass. For heterotrophic prokaryotes, conversion to carbon units were done considering 20 fg C $cell^{-1}$ (Lee and Fuhrman, 1987) and for heterotrophic nanoflagellates assuming 220 fg C μm^{-3} (Børsheim and Bratbak, 1987), a spherical shape and a diameter of 3 μm. The ratio of autotrophic and heterotrophic biomass during the experiments was used to evaluate the trophic status of the investigated communities and its evolution. Finally, a proxy for micro-phytoplankton biomass (B_{micro}) was estimated following Vidussi et al. (2001), as the sum of Fucoxanthin and Peridinin.

3. Results

3.1. Initial conditions

Initial conditions of various measured parameters at the three sampling stations while filling the tanks are shown in Table 2. pH_T and total alkalinity concentrations observed when pumping seawater for the experiments (before ^{13}C-bicarbonate addition and dust seeding: t-12h) followed a west to east increasing gradient (8.03, 8.04 and 8.07; 2443, 2529 and 2627 µmol kg^{-1} at FAST, TYR and ION, respectively). NO_x concentrations were maximal at station FAST with a NO_x:DIP molar ratio of ~ 4.6. Very low NO_x concentrations were observed at stations TYR and ION (14 and 18 nmol L^{-1}, respectively). DIP concentrations were the highest at station TYR (17 nmol L^{-1}) and the lowest at the most eastern station (ION, 7 nmol L^{-1}). Consequently, the lowest NO_x:DIP ratio was measured at TYR (0.8), compared to ION and FAST (2.8 and 4.6, respectively). Ammonium concentrations were maximal at TYR (0.045 µmol L^{-1}), intermediate at ION (0.022 µmol L^{-1}), and minimal at FAST (below detection limit). Silicate concentrations were similar at stations TYR and ION (~ 1 µmol L^{-1}) and higher than at station FAST (0.64 µmol L^{-1}).

Very low and similar concentrations of chlorophyll *a* were measured at the three stations (0.063 - 0.072 µg L^{-1}). The proportion of the different major pigments (Fig. 3) showed that phytoplankton communities at stations TYR and ION were very similar with a dominance of Prymnesiophytes (i.e. 19'-hexanoyloxyfucoxanthin; Ras et al., 2008) followed by Cyanobacteria (i.e. Zeaxanthin; Ras et al., 2008). In contrast, at station FAST, the planktonic community was clearly dominated by photosynthetic prokaryotes (i.e. Zeaxanthin and Divinyl-chlorophyll *a*; Cyanobacteria and Prochlorophytes, respectively; Ras et al., 2008). At all three stations, the

proportion of pigments representative of larger species (i.e. Fucoxanthin and Peridinin; diatoms and dinoflagellates respectively; Ras et al., 2008) were very small (< 5%).

Cellular abundances of all studied microorganisms (phytoplankton, micro-grazers, heterotrophic bacteria) were the highest at FAST (Table 2). Picoeukaryotes, *Synechococcus* and heterotrophic prokaryotes abundances followed an east to west increasing trend (ION < TYR < FAST). In contrast, nano-eukaryotes abundance was similar at FAST and ION, and minimal at TYR. The abundance of heterotrophic nanoflagellates (HNF) were similar at TYR and FAST (~110-125 cells mL^{-1}), twice as high as the one observed at station ION. This east to west increasing trend was also observed for micro-phytoplankton and micro-heterotrophs abundances (microscopic analyses; Table 2). The ratio between autotrophic biomass and heterotrophic biomass was clearly in favor of the heterotrophic compartment at stations TYR and FAST (~0.6 at the two stations) but the opposite was found at station ION (ca. 1.3).

3.2. Experimental conditions

Irradiance levels during the experiments in controls were maximal at station ION and minimal at station FAST (daily average maximum levels in controls: ~ 1050, ~ 1130 and ~ 1020 µmol photons m^{-2} s^{-1} at TYR, ION and FAST, respectively; Fig. 4). Decreases of water transparency after dust addition was observed at all three stations with a maximum dust impact at station ION and the lowest impact at station FAST where irradiance levels decreased by only 60 µmol photons m^{-2} s^{-1} after dust addition (average between tanks D and G). At station TYR, a more pronounced decrease was observed in acidified and warmed tanks (G1 and G2) with a decrease of daily average maximum irradiance of ~ 60 and ~ 160 µmol photons m^{-2} s^{-1} as compared to dust-amended tanks D and controls, respectively. Temperature control (Fig. 4) was not optimal showing deviations between replicates of treatment G of up to 1.5 °C (station ION). Temperature in controls and D

tanks displayed a daily cycle with an increase during the day and a decrease at night. Overall, the differences between the warmed treatment (G) and the other tanks were +3, +3.2 and +3.6 °C at TYR, ION and FAST, respectively.

Addition of CO_2-saturated filtered seawater led to a decrease of pH_T from 8.05 ± 0.004 (average ± SD between C1, C2, D1 and D2 at t0) to 7.74 (average between G1 and G2) at station TYR, from 8.07 ± 0.002 to 7.78 at station ION and 8.05 ± 0.001 to 7.72 at station FAST (Fig. 5). pH_T levels remained more or less constant in ambient pH levels tanks during all three experiments with no clear impact of dust addition in tanks D1 and D2. In lowered pH tanks, pH levels gradually increased during the experiments with a systematic larger increase in one of the duplicates (G1). Yet pH_T increases remained moderate thanks to the flushing of CO_2-enriched air above the tanks (pCO_2 of 1017 ± 11, 983 ± 96, 1023 ± 25 ppm at TYR, ION and FAST, respectively; data not shown). Partial pressure of CO_2 in ambient air was similar at the three stations, i.e. 410 ppm (data not shown). At all three stations, ^{13}C-addition led to an increase of total alkalinity between 6 and 11 µmol kg^{-1} and dust addition led to a decrease in tanks D and G between 8 and 16 µmol kg^{-1} with no apparent effects of warming and acidification. Overall, no large changes in this parameter were observed during the experiments (Fig. 5).

3.3. Changes in nutrient concentrations

Dust addition in tanks D and G led to a rapid and maximum input of NO_x (as observed during the first 6 h; Fig. 6; Table 3) of ~ 11 µmol L^{-1} at all three stations with no differences between both treatments. The corresponding dissolution percentage of N contained in the dust analog was between 94 and 99%. In contrast, maximum DIP release (within 6 h after dust addition) from the dust analog was much smaller and comprised between 20 and 37 nmol L^{-1}, with slightly higher release at FAST (31-37 nmol L^{-1}) as compared to the other stations. Dissolution percentages

399 for DIP were estimated between 9.2 and 17.3% of total phosphorus contained in dust. As a
400 consequence of these contrasted dissolution of N and P, NO_x:DIP ratios increased from initial
401 values below 5 to above 300, within 6 h after dust seeding, in the dust amended (D and G) tanks
402 (Fig. 6).

403 After these rapid increases due to N and P releases in dust amended tanks, both variables
404 decreased with time. While nutrient variability was small in control tanks over the duration of the
405 experiments (NO_x and DIP variations below 20 and 3 nmol L^{-1}, respectively), large decrease of both
406 elements was measured in dust amended tanks (D and G; Table 4). For NO_x, similar linear
407 decreases were observed throughout the experiments at stations TYR and ION with no visible
408 differences between tanks D and G. In contrast, at station FAST, a more pronounced decrease in
409 NO_x was observed in dust-amended (D and G) tanks as compared to the other stations, with
410 detectable larger decreases in warmed and acidified tanks relative to the D treatment. Nevertheless,
411 at all stations, NO_x concentrations in D and G treatments remained far above ambient levels
412 throughout the experiments (> 9 µmol L^{-1}). Abrupt decreases in DIP were observed during the three
413 experiments after the initial increase. At station TYR, after 24 h, all DIP released from dust
414 decreased to initial levels in tanks G while it took two more days to reach initial levels in tanks D.
415 In contrast, at station ION, no clear difference in DIP dynamics was observed between treatments D
416 and G, with concentrations that decreased rapidly during the first 24 h but that remained above
417 initial levels until the end of the experiment. At station FAST, similarly to station TYR, DIP
418 decreased rapidly from t12h in treatment G, reaching levels close to initial conditions at the end of
419 the experiment. DIP decrease was much lower in treatment D (Table 4) with concentrations
420 maintained far above ambient levels throughout the experiment. As a consequence of these
421 differences between NO_x and DIP dynamics as well as differences among stations, NO_x:DIP ratio

increased during the experiments with clear differences between stations (Fig. 6) and remained much higher than that in the controls over the duration of the three experiments.

Silicate dynamics showed at all stations higher concentrations in dust amended (D and G) tanks relative to the controls. At TYR, while in control tanks, concentrations remained stable, they increased linearly with time in the other tanks (D and G) with no apparent effect of the imposed increase in temperature and decrease in pH (i.e. tanks G). Difference of $Si(OH)_4$ concentration between dust amended treatments (D and G) and controls was ~0.1 µmol L^{-1} at the end of the experiment. At station ION, after an initial decrease of concentrations between t-12h and t0, concentrations increased in all tanks until the end of the experiment with higher concentration in dust amended tanks (D and G) than in controls (no difference between D and G treatments). In contrast, at FAST, concentrations increased between t-12h and t0, and continued to increase in all tanks (with higher values in dust amended tanks) until t48h and then decreased until the end of the experiment. At the end of the experiment (t96h), $Si(OH)_4$ concentration was higher in the G treatment than in the D treatment which was similar to the controls.

3.4. Changes in biological stocks

Regarding biological stocks, temporal dynamics showed very different patterns with respect to the sampling station. At TYR, total chlorophyll *a* concentrations did not change in dust amended tanks maintained under ambient levels of temperature and pH (Fig. 7) and even led to slightly decreased values 24 h after dust addition (e.g. -35 to -38% in D1 and D2, respectively as compared to controls; Table 5). No clear effect of dust addition (tanks D vs. C) were detectable for all groups based on pigment analyses (Fig. 7). Results obtained based on flow cytometry counting (Fig. 8) were coherent with these observations and showed stronger decreases in cell abundances for < 20 µm autotrophic groups in tanks D1 and D2 (-77 to -80%). In contrast, at this station, the abundance

of heterotrophic prokaryotes (HP) increased rapidly after dust addition both under ambient (+53-68%) and future (+68%) environmental conditions, with no clear difference among those treatments. In warmed and acidified tanks, strong discrepancies between the duplicates were observed for pigments and autotrophic cell abundances. Indeed, tank G1 showed moderately higher levels for all variables as compared to tanks C at the exception of pico-eukaryotes, while in G2 all variables responded strongly to dust addition with maximum relative changes of > 300% (at the exception of nano-eukaryotes: +119%). While HNF abundances responded positively to the treatments in D1, D2 and G2 (+100-352%), abundances increased sharply in tank G1 towards the end of the experiment (+1095%). At ION, a clear distinction between treatments could be observed for almost all pigments and cell abundances (Fig. 7, Fig. 8). At the exception of nano-eukaryotes and HNF, all variables (pigments and cell abundances) increased as a response to both dust addition and warmed/acidified conditions (i.e. C < D < G). As an example (Table 5), the maximum relative changes as compared to controls observed for total chlorophyll *a* were 109-183% and 399-426% in tanks D and G, respectively. The highest stimulation to dust addition was observed for *Synechococcus* with a +317-390% increase and +805-1425% increase in D and G tanks respectively (Table 5). Abundances of nano-eukaryotes and HNF suggested no impact of dust addition under ambient conditions but a positive impact in treatment G. In contrast to what was observed at TYR for HP abundances, an effect of temperature and pH was observed at station ION with a higher impact of dust addition under future environmental conditions. At station FAST, all above mentioned variables related to biological stocks increased strongly after dust addition (Fig. 7, Fig. 8 and Table 5). For instance, total chlorophyll *a* increased following an exponential trend until the end of the experiment reaching maximal values at t96h with slightly lower values observed under ambient environmental conditions (+237-318% in D tanks vs. ~ +400% in G tanks). Prymnesiophytes (i.e. 19'-hexanoyloxyfucoxanthin) and diatoms (i.e. Fucoxanthin) appeared as the

groups benefiting the most from dust addition with no large impacts of warming/acidification. In contrast, Pelagophytes (i.e. 19'-butanoyloxyfucoxanthin) and green algae (i.e. Total Chlorophyll *b*) responded much more in treatment G than in treatment D. Finally, although Cyanobacteria (i.e. Zeaxanthin) responded faster to dust addition under future environmental conditions (tanks G), this effect tended to attenuate towards the end of the experiment. In contrast to estimates based on HPLC data, increases in cell abundances did not generally take place until the end of the experiment. While abundances in pico-eukaryotes increased until t96h in treatment D, abundances sharply declined between t72h and t96h for this group in treatment G. The same trend was observed for *Synechococcus* during this experiment, although discrepancies between duplicates in treatment D at sampling time t96h did not allow drawing conclusions on the behavior of this group at the end of the experiment. Both under ambient and future conditions, abundances of nano-eukaryotes declined sharply between t72h and t96h. The decline in HP abundances appeared even earlier during the experiment with moderate maximum relative differences as compared to controls observed at t48h. HP abundances declined very sharply between t48h and t96h in treatment G, reaching control levels, while this decline was less sharp under ambient environmental levels. Finally, HNF dynamics during this experiment was hard to evaluate with no clear effects of dust addition or pH/temperature conditions and with a large increase in abundances in only one duplicate of treatment G (t24h) followed by a gradual decrease.

Abundances of meso-zooplankton at the end of the experiments showed relatively similar values at stations TYR and ION while much higher levels were observed at station FAST (Fig. 9). As a consequence of large variability between duplicates at stations TYR and ION, no clear effects of treatments were detected. At station FAST, although the sample size was too low to statistically test for differences, higher total abundances of meso-zooplankton species were observed in the dust-amended tanks with no differences between ambient and future conditions of temperature and

493 pH. However, differences in abundance were visible between these two treatments for specific
494 groups, with respectively higher abundance of Harosa and lower abundance of Crustacea (other
495 than copepods) and Mollusca in warmed and acidified tanks.

4. Discussion

4.1. Initial conditions

Overall, the three experiments were conducted with surface seawater collected during typical stratified oligotrophic conditions typical of the open Mediterranean Sea at this period of the year. However, at all three stations, initial concentrations of NO_x (14, 18 and 59 nmol L^{-1} at TYR, ION and FAST, respectively; Table 2) were lower that the ones reported by Manca et al. (2004) in surface waters (5 m) in these areas in spring (0.036 ± 0.10, 0.275 ± 0.358 and 0.183 ± 0.282 µmol L^{-1} for the areas corresponding to TYR, ION and FAST, respectively; http://doga.ogs.trieste.it/medar/climatologies/, last access: 28/04/2020). Similarly, surface DIP concentrations as measured at the three stations were lower than values extracted from the compilation of Manca et al. (2004) for the same period (0.072 ± 0.072, 0.054 ± 0.035 and 0.115 ± 0.078 µmol L^{-1} in the areas corresponding to TYR, ION and FAST, respectively). However, direct measurements of NO_x and DIP concentrations using nanomolar techniques (as performed in our study) are scarce in the Mediterranean Sea, limiting our ability to compare our results with these published values which, in any case, show large interannual variability. Djaoudi et al. (2018) reported low DIP values in the three studied basins. Furthermore, low observed concentrations of NO_x and DIP at all three stations during our study were also in agreement with reported concentrations in the coastal waters of Corsica during experiments using *in situ* mesocosms in June, whether during the DUNE project (DIP ~5 nmol L^{-1}; Pulido-Villena et al., 2014; NO_x < 30 nmol L^{-1}; Ridame et al., 2014) or during the MedSeA project (NO_x ~ 50 nmol L^{-1} and DIP ~ 35 nmol L^{-1}; Louis et al., 2017b). Furthermore, at all three stations, NO_x:DIP molar ratios were well below the Redfield ratio (16:1) and are consistent with ratios found in these previously cited studies. Both low NO_x:DIP ratio and low nutrient concentrations suggest that communities found at the three stations

519 experienced N and P co-limitation at the start of the experiments, as previously shown by Tanaka et
520 al. (2011). Some enrichment experiments in DIP, NO_3+NH_4, glucose, alone or in combinations were
521 conducted using seawater sampled while filling the tanks. Bacterial production was mainly
522 stimulated by N+P addition at the three sites, although a slight stimulation was also detected after P
523 addition alone at TYR and ION (France Van Wambeke, pers. comm.). Initial concentrations of
524 dissolved Fe in the sampled seawater ranged from 1.5 nmol L^{-1} (TYR) to 2.5 nmol L^{-1} (ION;
525 Roy-Barman et al., in preparation, this issue). Such concentrations were unlikely limiting for
526 biological activity as previously shown in the Mediterranean Sea (Bonnet et al., 2005; Ridame et
527 al., 2014).
528 Total chlorophyll *a* concentrations of ~ 0.06 - 0.07 µg L^{-1} (Table 2) were typical of
529 chlorophyll *a* levels found in these areas of the surface Mediterranean Sea at this period of the year,
530 as seen by satellite (Bosc et al., 2004), or from a database of *in situ* measurements (Manca et al.,
531 2004). During the DUNE and MedSeA projects cited above, chlorophyll *a* concentrations around
532 0.07 µg L^{-1} were also encountered at the start of these experiments conducted in coastal waters
533 (Gazeau et al., 2017; Ridame et al., 2014). Although total chlorophyll *a* concentrations were rather
534 similar between the three tested stations, the composition of the phytoplankton communities, based
535 on HPLC pigment analyses, differed substantially. Indeed, while the communities were dominated
536 by nano-eukaryotic species at stations TYR and ION, both HPLC and flow cytometry data suggest
537 a larger contribution of pico-eukaryotes and Cyanobacteria at station FAST. Micro-autotrophs (e.g.
538 large diatoms and dinoflagellates) were slightly higher at station FAST. Due to their low
539 competitiveness during periods of nutrient limitation, the small contribution of large phytoplankton
540 cells at the start of the experiment is a fingerprint of LNLC areas and surface Mediterranean waters
541 at this period of the year (Siokou-Frangou et al., 2010). Autotrophic biomasses, as estimated based
542 on flow cytometry data (see Material and Methods) were similar at station TYR and ION (5.6 and

543 6.0 µg C L^{-1}) and maximal at FAST (7.7 µg C L^{-1}; Table 2). Although these estimates do not take
544 into account the contribution of micro-autotrophs, they appear to be in fair agreement with
545 estimates based on total chlorophyll *a* data, assuming a carbon to chlorophyll ratio of 70 (Bellacicco
546 et al., 2016), i.e. 4.4, 4.6 and 5.1 µg C L^{-1} at TYR, ION and FAST, respectively. Furthermore, as
547 already mentioned, based on pigment analyses (HPLC), the sum of Fucoxanthin and Peridinin
548 (representative of diatoms and dinoflagellates, respectively) represented only ~10% of the total
549 chlorophyll *a* biomass at all stations. As biomass of both heterotrophic nanoflagellates and
550 prokaryotes followed a west to east gradient (FAST > TYR > ION), ratio of autotrophic vs
551 heterotrophic biomass appeared clearly in favor of the heterotrophic compartment at stations TYR
552 and FAST (ratio of 0.6) while a value above the metabolic balance was estimated at ION (ratio of
553 1.3). This is coherent with the highest net community production (NCP) rates being reported at this
554 station by Gazeau et al. (in preparation, this issue) showing that the initial community at the start of
555 this experiment was very close to metabolic balance (mean ± SE: -0.06 ± 0.09 µmol O_2 L^{-1} d^{-1}). The
556 highest community respiration rates and consequently lowest NCP rates were measured at station
557 TYR (-1.9 µmol O_2 L^{-1} d^{-1}) further suggesting that the autotrophic plankton community was not
558 very active (Ridame et al., in preparation, this issue) also confirmed by the lowest rate of CO_2
559 fixation; Ridame et al., in preparation, this issue), and relying on regenerated nutrients, as shown by
560 the highest level of NH_4^+ measured at the start of this experiment. In contrast, the community at
561 station FAST although slightly heterotrophic (Gazeau et al., in preparation, this issue) and limited
562 by the low amount of nutrients (Table 2) was the most active as shown by the highest levels of ^{14}C
563 production and heterotrophic prokaryote production (Gazeau et al., in preparation, this issue) as
564 well as N_2 fixation (Ridame et al., in preparation, this issue). Altogether, the heterotrophic signature
565 of the three investigated stations, although closer to metabolic balance for ION, reflected typical

natural biogeochemical conditions in the Mediterranean Sea during late spring to early summer (Regaudie-de-Gioux et al., 2009).

4.2. Experimental assessment

The experimental tanks used in this study have already been validated in several studies designed to investigate the inputs of macro- and micro-nutrients (e.g. NO_x, DIP, DFe) and the export of organic matter, under close-to-abiotic conditions (seawater filtration onto 0.2 µm) following simulated wet dust events using the same analog as used in our study (Bressac and Guieu, 2013; Louis et al., 2017a, 2018). Louis et al. (2017a, 2018) further investigated these impacts under lowered pH conditions. During these experiments, no control of atmospheric pCO_2 was performed and pH levels in the acidified filtered seawater rapidly increased due to CO_2 degassing (from ~7.4 to ~7.7 in six days). Prior to the cruise, we improved our experimental system to allow mimicking future conditions by controlling atmospheric pCO_2 in addition to light and temperature (i.e. climate reactors). During our experiments, thanks to the control of atmospheric pCO_2 (~ 1000 ppm), we significantly reduced CO_2 degassing and maintained pH levels close to experimental targets. However, as can be seen in Fig. 5, the regulation was consistently more efficient in tank G2 as compared to G1. We attribute this small discrepancy (highest difference of 0.04 pH units between the two G tanks at FAST) to a potential leak or a longer flushing time above tank G1. Nevertheless, we do not anticipate this as an issue.

The lids above tanks, equipped with LEDs in order to reproduce sunlight intensity and spectrum, were used for the first time during these experiments. The maximal intensity reached under control conditions (C1, C2) was between 900 and 1000 µmol photons m^{-2} d^{-1}. Although slightly lower than estimates for the Northwestern Mediterranean Sea at 5 m depth in June (~1100 µmol photons m^{-2} d^{-1}; Bernard Gentili, personal communication, 2017), simulated intensities were

589 fairly consistent between duplicates under control conditions (C1, C2) and under dust-amended
590 conditions (D1, D2). In contrast, larger differences were observed between warmed and acidified
591 tanks (G1 and G2; maximal differences of 100-200 µmol photons m^{-2} d^{-1} depending on the
592 experiment) that generally increased during each experiment. The reasons of these discrepancies are
593 not clear and could result from differences of light intensity generated by the lids, of PAR sensors
594 sensitivity and/or of the amount of particles remaining in the tanks. Unfortunately, although
595 replication appeared satisfactory for this treatment (except at station TYR; see below), we can not
596 fully exclude a potential impact of these technical issues on our results for this warmer and acidified
597 treatment. A similar conclusion can be drawn regarding temperature regulation in the container
598 where temperature was not spatially homogeneous, leading to significant differences among
599 replicates. After this study, experimental tanks were installed in a new container in order to solve
600 these problems.

601 The experimental strategy chosen during this study implied considering three different
602 treatments: control, simulation of dust deposition and simulation of dust deposition under future
603 projected environmental conditions. This unbalanced design, i.e. without the consideration of a
604 treatment without dust addition under future temperature and pH levels, was chosen for practical
605 reasons as only six tanks could be used for this study. Furthermore, as already mentioned, previous
606 experiments clearly showed very limited effects of these drivers when communities are strongly
607 limited by nutrient availability (Maugendre et al., 2017), therefore the objective of our study was to
608 test the impact of an external forcing (atmospheric deposition) under future conditions, without
609 discriminating warming from acidification effects. More importantly, the relatively low number of
610 experimental units that could be installed in an ambarcable clean container, implied considering
611 duplicated tanks for each treatment. This forced choice implied the impossibility to perform
612 statistical analyses on our results, as at least triplicates are necessary for most statistical tests.

Differences between duplicates were, for the vast majority of studied variables and processes, lower than differences between treatments and appear acceptable considering the difficulty to incubate plankton communities for which slight differences in their initial composition can translate into very important differences in dynamics (Eggers et al., 2014). Unfortunately, while no large replication issues were observed during the ION and FAST experiments, very important discrepancies were detected for tanks of the warmed and acidified treatment at station TYR. The reasons behind the different behavior of the autotrophic community in tanks G1 and G2 are not fully understood but we strongly suspect that heterotrophic nano-flagellates, feeding mainly on prokaryotic picoplankton (Sherr and Sherr, 1994), exerted a strong top-down control on this group in tank G1 in which HNF abundance sharply increased during the experiment (+1100% in G1 vs. + 300% in G2). Interestingly, while autotrophic prokaryotes were clearly impacted, no differences between the two tanks G1 and G2 were observed for heterotrophic prokaryotes although nanoflagellates are known to feed to this group as well (Sherr and Sherr, 1994). Heterotrophic nano-flagellates were likely not the only group of grazers which abundance increased during this experiment in tank G1 as the biomass of diatoms (i.e. Fucoxanthin) did not increase in this tank. Nevertheless, as no analyses of micro-grazer abundances were performed during the experiments, this hypothesis can not be verified. All in all, these discrepancies for this treatment at station TYR remain an issue and prevent us from drawing any conclusion on the combined effect of temperature and pH on the dynamics of the community for that station.

4.3. Impact of dust addition

During the three experiments, the observed increases in NO_x and DIP few hours after dust addition were rather similar to the enrichment levels obtained during the DUNE experiments at the surface of the mesocosms (~ 50 m^3) after the simulation of a wet dust deposition using the same

dust analog and the same simulated flux (Pulido-Villena et al., 2014; Ridame et al., 2014). NO_x levels moderately decreased over the course of our experiments due to biological uptake (50-1420 nmol L^{-1}, depending on the experiment). The opposite feature was observed for the DIP released by dust that rapidly decreased during our experiments except at station FAST in the D treatment where final concentrations did not reach initial levels. These enrichment levels, especially for NO_x, were much higher than those observed by Pitta et al. (2017, and references therein) during land-based mesocosm experiments in the Eastern Mediterranean Sea, in which a dry Saharan deposition was simulated. In contrast to this experiment, the objective of our study was to assess the impact of wet dust deposition, the main dust deposition pathway in the Western Mediterranean Sea (Loÿe-Pilot and Martin, 1996). Furthermore, following observations of mixing between dust and polluted air masses during their transport (e.g. Falkovich et al., 2001; Putaud et al., 2004), we chose to use an evapo-condensed dust analog that mimics the processes taking place in the atmosphere prior to deposition, essentially the adsorption of inorganic and organic soluble species (e.g. sulfate and nitrate; see Guieu et al., 2010a, for further details). The imposed evapo-condensation processes are responsible for the large nitrate releasing capacity of the dust particles used in our study. Regarding the intensity of simulated wet deposition event, the 10 g m^{-2} deposition event considered here represents a high but realistic scenario, as several studies reported even higher short deposition events in this area of the Mediterranean Sea (Bonnet and Guieu, 2006; Loÿe-Pilot and Martin, 1996; Ternon et al., 2010).

Although NO_x and DIP increases after dust addition were rather similar during our three experiments, interestingly the impacts on plankton community composition and functioning were drastically different. Most experiments reporting on the effect of dust addition in the Mediterranean Sea showed significant increases in chlorophyll *a* concentrations (mean 89% increase; Guieu and Ridame, 2020). Such fertilization of primary producers was indeed observed at stations ION and

FAST under present conditions (maximum change in total chlorophyll *a* relative to the controls was ~280% at FAST and ~150% at ION). The largest increase in chlorophyll *a* concentrations at station FAST is coherent with the largest observed NO_x decrease following dust addition at this station. Interestingly, following dust addition at this station, autotrophic production did not lead to DIP exhaustion throughout the experiment as DIP concentrations were still above ambient conditions at the end of the experiment. Maximal primary production rates (^{14}C-incorporation) at this station at the end of the experiment suggest a strong DIP recycling and the dominance of regenerated production towards the end of the experiment (Gazeau et al., in preparation, this issue). Guieu et al. (2014b) showed, based on the analysis of eight aerosols addition studies, that *Synechococcus* had in most of the cases a weak responses to aerosol addition in contrast to nano- and micro-phytoplankton, suggesting that aerosol deposition may lead to an increase in larger size class phytoplankton. Yet, *Synechococcus* were well stimulated in some dust addition experiments (Herut et al., 2005; Lagaria et al., 2017; Paytan et al., 2009), similar to what was observed at both stations ION and FAST, where *Synechococcus* abundance was clearly enhanced by dust deposition. The increase in *Synechococcus* abundance to dust-amended tanks was the highest relative to those of pico- and nano-eukaryotes at these stations. This was especially true at station ION where no clear response to nutrient enrichment was observed for nano-eukaryotes throughout the experiment. However, it must be stressed that our experiments were performed over a relatively short period (3 to 4 days), and the sharp increase in Fucoxanthin paralleled by a decrease in silicates, at the end of the experiment at station FAST where DIP limitation was not yet apparent, suggests a delayed response of diatoms as compared to smaller groups (i.e. autotrophic prokaryotes, pico- and nano-eukaryotes). Although this was not observed based on pigment analyses, the sharp decline in nano-eukaryote abundances at the end of the FAST experiment following dust addition, further

683 suggests that this group, reacting quickly to nutrient enrichment was progressively grazed and/or
684 outcompeted by larger phytoplankton species.

685 In contrast to what was observed at stations ION and FAST, no stimulation of autotrophic
686 biomass and primary production rates (Gazeau et al., in preparation, this issue) was observed in the
687 dust treatments under present conditions at station TYR. To the best of our knowledge, this is the
688 first experimental evidence of a complete absence of response from an autotrophic community
689 following dust wet deposition. There is clear evidence that not only phytoplankton but also
690 heterotrophic bacteria are limited by inorganic nutrients, mainly DIP, in oligotrophic systems
691 (Obernosterer et al., 2003; Wambeke et al., 2002), thus suggesting that the supply of these resources
692 could explain variability in bacterial activity. Many recent studies have shown significant increase
693 in heterotrophic bacterial abundance, respiration and/or production following dust deposition in
694 oligotrophic ecosystems (Lekunberri et al., 2010; Pitta et al., 2017; Pulido-Villena et al., 2008,
695 2014; Romero et al., 2011). Most of the time, heterotrophic processes appear to be more stimulated
696 by dust pulses compared to autotrophic processes with increasing degree of oligotrophy, the
697 dominant response being modulated by the competition for nutrients between phytoplankton and
698 bacteria (Marañón et al., 2010). This is clearly what was observed at this station, with heterotrophic
699 prokaryotes reacting quickly and strongly to nutrient addition both in terms of abundances (max: +
700 53-68%) and production rates (max: + 787-946%; Gazeau et al., in preparation, this issue). The
701 absence of response from autotrophic stocks could be due to a tight top-down control from grazers
702 hiding potential responses from the autotrophic community (Lekunberri et al., 2010; Marañón et al.,
703 2010). Feliu et al. (2020, this issue) have shown that the mesozooplankton assemblage at TYR was
704 clearly impacted by a dust event that took place nine days before sampling at that station (François
705 Dulac, Pers. Com. 2019) and evidenced by dust export in *in situ* deployed sediment traps (Bressac
706 et al., in preparation, this issue). This dust deposition likely stimulated phytoplankton growth and

consequently increased the abundance of herbivorous grazers (copepods) and attracted carnivorous species. After the rapid increase observed a few hours after dust addition, DIP levels decreased to reach similar levels than in control tanks at the end of this experiment (Fig. 6). Yet, heterotrophic prokaryote abundances increased until the end of the experiment (Fig. 8) although production rates reached a plateau after 24 h (Gazeau et al., in preparation, this issue). This is coherent with measurements of the alkaline phosphatase activity that slightly increased at the end of the experiment in dust-amended tanks suggesting the use of dissolved organic phosphorus by bacteria to compensate for the increasing lack of DIP (Gazeau et al., in preparation, this issue). Altogether, the strong stimulation of heterotrophic prokaryotes and the absence of detectable effects on the autotrophic compartment drove the community towards a stronger net heterotrophic state as shown by increases in community respiration and decreases in net community production rates in dust-amended as compared to control tanks (Gazeau et al., in preparation, this issue).

At station FAST, the competition for nutrients between autotrophs and heterotrophs was clearly in favor of autotrophs. While, as discussed above, all groups of primary producers benefited from nutrient enrichment at this station, the increases in heterotrophic prokaryote abundances were rather limited following dust deposition, leading to an increase of net community production rates throughout this experiment to reach positive levels while control tanks remained below metabolic balance (Gazeau et al., in preparation, this issue). At station ION, the situation was somewhat intermediate with a parallel enhancement of both autotrophic and heterotrophic stocks and processes, although the system was slightly in favor of net autotrophy at the end of the experiment (Gazeau et al., in preparation, this issue).

Transfer of newly produced organic matter to higher trophic levels in the different treatments was evaluated through the quantification of meso-zooplankton abundance at the end of each experiment. Although we are fully aware that such an approach is certainly criticizable

731 considering the low incubation times (3 to 4 days), it may still be representative of lowered
732 mortality or faster growth. Altogether it does not appear as a surprise that an increase in
733 meso-zooplankton abundances was only detected at station FAST where the strongest enhancement
734 of primary production was observed. Such an increase in meso-zooplankton abundance in the
735 dust-amended as compared to control treatment was observed during land-based mesocosm
736 experiments in the Eastern Mediterranean Sea (Pitta et al., 2017).

737 Finally, although no clear effects of dust deposition under present conditions were detectable
738 on autotrophic prokaryotes at station TYR, the strongest increase in N_2 fixation rates was recorded
739 at this station (+434-503%, as compared to +173-256% and +41-49% at ION and FAST,
740 respectively; see Ridame et al., in preparation, this issue, for more details). However, the potential
741 impact of this process on NO_x concentration is highly negligible compared to the very large stock of
742 NO_x present in the dust-amended tanks, as less than 1 nmol L^{-1} d^{-1} of NO_x can be produced by this
743 process (Ridame et al., in preparation, this issue).

744 4.4. Impact of warming and acidification

745 Very few past studies have investigated the release and fate of nutrients from atmospheric
746 particles under climate conditions as expected for the end of the century, and, to the best of our
747 knowledge, our study represents the first attempt to test for the combined effect of ocean warming
748 and acidification on these processes. Louis et al. (2018) have already shown from an abiotic dust
749 experiment that even an extreme ocean acidification scenario (~ -0.6 pH units) does not impact the
750 bioavailability of macro- and micro-nutrients (NO_x, DIP and DFe) for surface phytoplankton
751 communities in the oligotrophic Northwestern Mediterranean Sea, using the same dust analog and
752 simulated flux as used during our experiments. Similar results were presented by Mélançon et al.
753 (2016) regarding the release of DFe from dust in high-nutrient low-chlorophyll (HNLC) waters of

754 the Northeastern Pacific, following a mild ocean acidification scenario of -0.2 pH units. Our results
755 agree with these previous findings and further highlighted the absence of direct effect of ocean
756 warming (+3 °C) on the release of nutrients from atmospheric particles.

757 The differences in nutrient consumption dynamics between ambient and warmed/acidified
758 tanks were substantially dependent on the considered nutrient and investigated station. Regarding
759 NO_x, while no impacts of warming and acidification could be observed at stations TYR and ION
760 due to large variability between the duplicates (Table 4), larger NO_x consumption rates were shown
761 under future climate conditions at the most productive station FAST as a consequence of strongly
762 enhanced biological stocks (see thereafter) and metabolic rates (Gazeau et al., in preparation, this
763 issue). The differences in DIP dynamics between the two dust-amended treatments were more
764 complex to interpret depending on the investigated station. A clear feature of our experiments is
765 that, in contrast to present day pH and temperature conditions, all the stock of DIP released from
766 dust was consumed at the end of the three experiments under future conditions. That being said, the
767 decreasing rates of DIP concentrations for that future conditions treatment differed depending on
768 the station (Table 4). While DIP dynamics were relatively similar between treatments at ION, a
769 clear effect of warming and acidification was shown at station TYR and FAST where the vast
770 majority of released DIP was consumed within 24 h (ΔDIP = -1.3 and -1.1 to -1.5 nmol L^{-1} h^{-1} at
771 TYR and FAST, respectively). An interesting outcome at station TYR was that, despite the
772 important discrepancies observed for autotrophic stocks and metabolic rates between the duplicates
773 G1 and G2 (see section 4.2), a very similar dynamics was observed for DIP concentrations in these
774 tanks. As heterotrophic prokaryote biomass and production rates (Gazeau et al., in preparation, this
775 issue) did not differ between these duplicate tanks, this further highlights the clear dominance of
776 heterotrophic processes at this station, a dominance which was exacerbated by dust addition and
777 future climate conditions.

At station ION, DIP consumption rates were similar following dust addition under present and future conditions. This results appears surprising as large impacts of warming and acidification have been observed, especially for primary producers, as shown by almost doubled chlorophyll *a* concentrations as compared to dust amended tanks (D). At this station, all autotrophic groups benefited from ocean acidification and warming. *Synechococcus* and to a lesser extent pico-eukaryotes appeared as the most impacted ones. Yet these differences of sensitivity among autotrophs did not lead to detectable changes in the composition of the autotrophic assemblage as compared to ambient conditions, with still a large dominance of nano-eukaryote carbon biomass at the end of this experiment (62% in treatment G vs. 64% in treatment D). Very contrasted results have been shown on the effect of ocean acidification on small autotrophic species (e.g. Dutkiewicz et al., 2015) while there are increasing evidences that small phytoplankton species will be favored in a warmer ocean (e.g. Chen et al., 2014; Daufresne et al., 2009; Morán et al., 2010). As mentioned earlier, our experimental protocol was not conceived to discriminate temperature from pH effects, however results concur with those of Maugendre et al. (2015) which further suggested temperature over elevated CO_2 as the main driver of increased picophytoplankton abundance. As heterotrophic prokaryotes were also positively impacted by future environmental conditions, the similarity of DIP dynamics between ambient and future conditions suggests a tight coupling between the autotrophic and heterotrophic compartments at this station. This is further evidenced by the absence of differences detected over the relatively short time duration of our experiment on meso-zooplankton abundance and carbon export efficiency (Gazeau et al., in preparation, this issue).

At FAST, similar to what was observed at station ION, all phytoplanktonic groups were positively impacted by warming and acidification with the strongest changes detected for *Synechococcus* as compared to ambient conditions. However, in contrast to station ION, all groups reached maximal abundances (and carbon biomass) after 3 days of incubations, thereafter

drastically decreasing most likely as a consequence of DIP limitation (see above). It must be stressed that this pattern could not be observed through pigment dynamics as no sampling was performed for these analyses after 3 days of incubation. Also, in contrast to station ION, the abundance of heterotrophic prokaryotes in the warmer and acidified treatment reached a maximum after 2 days of incubations and then strongly decreased to reach levels observed in the control treatment. This suggests that the heterotrophic compartment was the first to suffer from DIP limitation and further highlights the dominance of the autotrophic compartment in terms of nutrient consumption at this station. The differential dynamics of these two compartments under warmer and acidified conditions most likely led to an excess production of organic matter that translated, for instance, in higher dissolved organic carbon concentrations in this treatment (Gazeau et al., in preparation, this issue). This excess production as compared to ambient conditions did not seem to reach higher trophic levels as no clear differences in meso-zooplankton abundances were observed. We fully acknowledge that the duration of our experiments was certainly too short to carefully assess the proportion of newly formed organic matter consumed by meso-zooplanktonic species and its effect on their abundances, yet group-specific variations were observed. Finally, it appeared that at least part of this excess organic matter was exported to the bottom of the tanks as a higher carbon export efficiency was observed at this station under warmer and acidified conditions (Gazeau et al., in preparation, this issue).

5. Conclusion

These experiments conducted during the PEACETIME cruise represent the first attempt to investigate the impacts of atmospheric deposition on surface plankton communities both under present and future environmental conditions. Despite few experimental issues that are discussed, the three experiments provided new insights on these potential impacts in the open Mediterranean Sea. Interestingly, the effect of dust deposition was highly different between the three investigated stations in the Tyrrhenian Sea, Ionian Sea and in the Algerian basin. As the initial conditions in the sampled surface seawater at the three stations were very similar in terms of nutrient availability and chlorophyll content, these differences rather seem to be a consequence of the initial metabolic states of the community (autotrophy vs. heterotrophy). In all three cases, nutrient addition from dust deposition did not strongly modify but rather exacerbated this initial state. Relative changes in main parameters presented in this manuscript and processes presented in Gazeau et al. (in preparation, this issue) as a consequence of dust addition under present and future environmental conditions are shown in Fig. 10, and compared to the compilation of published data for the Mediterranean Sea from Guieu and Ridame (2020). At station TYR, under conditions of a clear dominance of heterotrophs on the use of resources, dust addition drove the community into an even more heterotrophic state with no detectable effect on primary producers. At station ION, where the community was initially closer to metabolic balance, both heterotrophic and autotrophic compartments benefited from dust derived nutrients. At FAST, the most active station in terms of autotrophic production, addition of nutrients boosted both compartments but heterotrophic prokaryotes became quickly P-limited and overall larger effects were observed for phytoplankton. Ocean acidification and warming did not have any detectable impact on the release of nutrients from atmospheric particles. Furthermore, these external drivers did not drastically modify the

composition of the autotrophic assemblage with all groups benefiting from warmer and acidified conditions. However, very large increases were observed both for autotrophic and heterotrophic stocks and processes suggesting an exacerbation of effects from atmospheric dust deposition in the future, rather than a change in the role of Mediterranean surface plankton community as a source or a sink of CO_2 to or from the atmosphere.

Data availability

All data and metadata will be made available at the French INSU/CNRS LEFE CYBER database (scientific coordinator: Hervé Claustre; data manager, webmaster: Catherine Schmechtig).

INSU/CNRS LEFE CYBER (2020)

Author contributions

FG and CG designed and supervised the study. FG, CG, CR and KD sampled seawater from the experimental tanks during the experiments. JMG and GDL participated in the technical preparation of the experimental system and all authors participated in sample analyses. FG, CR and CG wrote the paper with contributions from all authors.

Financial support

This study is a contribution to the PEACETIME project (http://peacetime-project.org), a joint initiative of the MERMEX and ChArMEx components supported by CNRS-INSU, IFREMER, CEA, and Météo-France as part of the programme MISTRALS coordinated by INSU. PEACETIME was endorsed as a process study by GEOTRACES. PEACETIME cruise (https://doi.org/10.17600/17000300).

Acknowledgments

The authors thank the captain and the crew of the RV Pourquoi Pas ? for their professionalism and their work at sea. We thank Julia Uitz, Céline Dimier and the SAPIGH HPLC analytical service at Institut de la Mer de Villefranche (IMEV) for sampling and analysis of phytoplankton pigments, John Dolan for microscopic countings as well as Lynne Macarez and the PIQv-platform of

868 EMBRC-France, a national Research Infrastructure supported by ANR, under the reference
869 ANR-10-INSB-02, for mesozooplankton analyses.

References

Aminot, A. and Kérouel, R.: Dosage automatique des nutriments dans les eaux marines : méthodes en flux continu, Editions Ifremer, méthodes d'analyse en milieu marin., 2007.

Behrenfeld, M. J., O'Malley, R. T., Siegel, D. A., McClain, C. R., Sarmiento, J. L., Feldman, G. C., Milligan, A. J., Falkowski, P. G., Letelier, R. M. and Boss, E. S.: Climate-driven trends in contemporary ocean productivity, Nature, 444(7120), 752–755, 2006.

Bellacicco, M., Volpe, G., Colella, S., Pitarch, J. and Santoleri, R.: Influence of photoacclimation on the phytoplankton seasonal cycle in the Mediterranean Sea as seen by satellite, Remote Sensing of Environment, 184, 595–604, doi:10.1016/j.rse.2016.08.004, 2016.

Bergametti, Gi., Dutot, A.-L., Buat-MéNard, P., Losno, R. and Remoudaki, E.: Seasonal variability of the elemental composition of atmospheric aerosol particles over the northwestern Mediterranean, Tellus B: Chemical and Physical Meteorology, 41(3), 353–361, doi:10.3402/tellusb.v41i3.15092, 1989.

Bonnet, S. and Guieu, C.: Atmospheric forcing on the annual iron cycle in the western Mediterranean Sea: A 1-year survey, Journal of Geophysical Research: Oceans, 111(C9), doi:10.1029/2005JC003213, 2006.

Bonnet, S., Guieu, C., Chiaverini, J., Ras, J. and Stock, A.: Effect of atmospheric nutrients on the autotrophic communities in a low nutrient, low chlorophyll system, Limnology and Oceanography, 50(6), 1810–1819, doi:10.4319/lo.2005.50.6.1810, 2005.

Børsheim, K. Y. and Bratbak, G.: Cell volume to cell carbon conversion factors for a bacterivorous Monas sp. enriched from seawater, Marine Ecology Progress Series, 36(2), 171–175, 1987.

Bosc, E., Bricaud, A. and Antoine, D.: Seasonal and interannual variability in algal biomass and primary production in the Mediterranean Sea, as derived from 4 years of SeaWiFS observations, Global Biogeochemical Cycles, 18(1), doi:10.1029/2003GB002034, 2004.

Bressac, M. and Guieu, C.: Post-depositional processes: What really happens to new atmospheric iron in the ocean's surface?, Global Biogeochemical Cycles, 27(3), 859–870, doi:10.1002/gbc.20076, 2013.

Bressac, M., Wagener, T., Tovar-Sanchez, A., Ridame, C., Albani, S., Fu, F., Desboeufs, K. and Guieu, C.: Residence time of dissolved and particulate trace elements in the surface Mediterranean Sea (Peacetime cruise), Biogeosciences, in preparation.

Bressac, M., Guieu, C., Doxaran, D., Bourrin, F., Desboeufs, K., Leblond, N. and Ridame, C.: Quantification of the lithogenic carbon pump following a simulated dust-deposition event in large mesocosms, Biogeosciences, 11(4), 1007–1020, doi:https://doi.org/10.5194/bg-11-1007-2014, 2014.

Chen, B., Liu, H., Huang, B. and Wang, J.: Temperature effects on the growth rate of marine picoplankton, Marine Ecology Progress Series, 505, 37–47, doi:10.3354/meps10773, 2014.

Christaki, U., Courties, C., Massana, R., Catala, P., Lebaron, P., Gasol, J. M. and Zubkov, M. V.: Optimized routine flow cytometric enumeration of heterotrophic flagellates using SYBR Green I, Limnology and Oceanography: Methods, 9(8), 329–339, doi:10.4319/lom.2011.9.329, 2011.

Daufresne, M., Lengfellner, K. and Sommer, U.: Global warming benefits the small in aquatic ecosystems, PNAS, 106(31), 12788–12793, doi:10.1073/pnas.0902080106, 2009.

912 Desboeufs, K., Leblond, N., Wagener, T., Bon Nguyen, E. and Guieu, C.: Chemical fate and settling
913 of mineral dust in surface seawater after atmospheric deposition observed from dust seeding
914 experiments in large mesocosms, Biogeosciences, 11(19), 5581–5594,
915 doi:https://doi.org/10.5194/bg-11-5581-2014, 2014.

916 Desboeufs, K., Bon Nguyen, E., Chevaillier, S., Triquet, S. and Dulac, F.: Fluxes and sources of
917 nutrient and trace metal atmospheric deposition in the northwestern Mediterranean,
918 Atmospheric Chemistry and Physics, 18(19), 14477–14492,
919 doi:https://doi.org/10.5194/acp-18-14477-2018, 2018.

920 Dickson, A. G., Sabine, C. L. and Christian, J. R.: Guide to best practices for ocean CO2
921 measurements, PICES, Sydney., 2007.

922 Djaoudi, K., Van Wambeke, F., Coppola, L., D'Ortenzio, F., Helias-Nunige, S., Raimbault, P.,
923 Taillandier, V., Testor, P., Wagener, T. and Pulido-Villena, E.: Sensitive Determination of the
924 Dissolved Phosphate Pool for an Improved Resolution of Its Vertical Variability in the
925 Surface Layer: New Views in the P-Depleted Mediterranean Sea, Front. Mar. Sci., 5,
926 doi:10.3389/fmars.2018.00234, 2018.

927 Duce, R. A., Liss, P. S., Merrill, J. T., Atlas, E. L., Buat-Menard, P., Hicks, B. B., Miller, J. M.,
928 Prospero, J. M., Arimoto, R., Church, T. M., Ellis, W., Galloway, J. N., Hansen, L., Jickells,
929 T. D., Knap, A. H., Reinhardt, K. H., Schneider, B., Soudine, A., Tokos, J. J., Tsunogai, S.,
930 Wollast, R. and Zhou, M.: The atmospheric input of trace species to the world ocean, Global
931 Biogeochemical Cycles, 5(3), 193–259, doi:10.1029/91GB01778, 1991.

932 Dutkiewicz, S., Morris, J. J., Follows, M. J., Scott, J., Levitan, O., Dyhrman, S. T. and
933 Berman-Frank, I.: Impact of ocean acidification on the structure of future phytoplankton

communities, Nature Climate change, 5, 1002–1006, doi:10.1038/nclimate2722, 2015.

Eggers, S. L., Lewandowska, A. M., Barcelos e Ramos, J., Blanco-Ameijeiras, S., Gallo, F. and Matthiessen, B.: Community composition has greater impact on the functioning of marine phytoplankton communities than ocean acidification, Global Change Biology, 20(3), 713–723, doi:10.1111/gcb.12421, 2014.

Emerson, S., Quay, P., Karl, D., Winn, C., Tupas, L. and Landry, M.: Experimental determination of the organic carbon flux from open-ocean surface waters, Nature, 389(6654), 951–954, doi:10.1038/40111, 1997.

Falkovich, A. H., Ganor, E., Levin, Z., Formenti, P. and Rudich, Y.: Chemical and mineralogical analysis of individual mineral dust particles, Journal of Geophysical Research: Atmospheres, 106(D16), 18029–18036, doi:10.1029/2000JD900430, 2001.

Feliú, G., Pagano, M., Hidalgo, P. and Carlotti, F.: Structure and functioning of epipelagic mesozooplankton and response to dust events during the spring PEACETIME cruise in the Mediterranean Sea, Biogeosciences Discussions, 1–35, doi:https://doi.org/10.5194/bg-2020-126, 2020.

Gazeau, F., Marañón, E., Van Wambeke, F., Alliouane, S., Stolpe, C., Blasco, T., Ridame, C., Pérez-Lorenzo, M., Engel, A., Zäncker, B. and Guieu, C.: Impact of dust enrichment on carbon budget and metabolism of Mediterranean plankton communities under present and future conditions of pH and temperature, Biogeosciences, in preparation.

Gazeau, F., Sallon, A., Pitta, P., Tsiola, A., Maugendre, L., Giani, M., Celussi, M., Pedrotti, M. L., Marro, S. and Guieu, C.: Limited impact of ocean acidification on phytoplankton community structure and carbon export in an oligotrophic environment: Results from two

short-term mesocosm studies in the Mediterranean Sea, Estuarine, Coastal and Shelf Science, 186, 72–88, doi:10.1016/j.ecss.2016.11.016, 2017.

Giovagnetti, V., Brunet, C., Conversano, F., Tramontano, F., Obernosterer, I., Ridame, C. and Guieu, C.: Assessing the role of dust deposition on phytoplankton ecophysiology and succession in a low-nutrient low-chlorophyll ecosystem: a mesocosm experiment in the Mediterranean Sea, Biogeosciences, 10(5), 2973–2991, doi:https://doi.org/10.5194/bg-10-2973-2013, 2013.

Gorsky, G., Ohman, M. D., Picheral, M., Gasparini, S., Stemmann, L., Romagnan, J.-B., Cawood, A., Pesant, S., García-Comas, C. and Prejger, F.: Digital zooplankton image analysis using the ZooScan integrated system, J Plankton Res, 32(3), 285–303, doi:10.1093/plankt/fbp124, 2010.

Guieu, C. and Ridame, C.: Impact of atmospheric deposition on marine chemistry and biogeochemistry, in Atmospheric Chemistry in the Mediterranean Region: Comprehensive Diagnosis and Impacts, edited by F. Dulac, S. Sauvage, and E. Hamonou, Springer, Cham, Switzerland., 2020.

Guieu, C., Dulac, F., Desboeufs, K., Wagener, T., Pulido-Villena, E., Grisoni, J.-M., Louis, F., Ridame, C., Blain, S., Brunet, C., Bon Nguyen, E., Tran, S., Labiadh, M. and Dominici, J.-M.: Large clean mesocosms and simulated dust deposition: a new methodology to investigate responses of marine oligotrophic ecosystems to atmospheric inputs, Biogeosciences, 7(9), 2765–2784, doi:https://doi.org/10.5194/bg-7-2765-2010, 2010a.

Guieu, C., Loye-Pilot, M. D., Benyahya, L. and Dufour, A.: Spatial variability of atmospheric fluxes of metals (Al, Fe, Cd, Zn and Pb) and phosphorus over the whole Mediterranean from

a one-year monitoring experiment: Biogeochemical implications, Marine Chemistry, 120(1–4), 164–178, doi:10.1016/j.marchem.2009.02.004, 2010b.

Guieu, C., Ridame, C., Pulido-Villena, E., Bressac, M., Desboeufs, K. and Dulac, F.: Impact of dust deposition on carbon budget: a tentative assessment from a mesocosm approach, Biogeosciences, 11(19), 5621–5635, 2014a.

Guieu, C., Aumont, O., Paytan, A., Bopp, L., Law, C. S., Mahowald, N., Achterberg, E. P., Marañón, E., Salihoglu, B., Crise, A., Wagener, T., Herut, B., Desboeufs, K., Kanakidou, M., Olgun, N., Peters, F., Pulido‐Villena, E., Tovar‐Sanchez, A. and Völker, C.: The significance of the episodic nature of atmospheric deposition to Low Nutrient Low Chlorophyll regions, Global Biogeochemical Cycles, 28(11), 1179–1198, doi:10.1002/2014GB004852, 2014b.

Guieu, C., D'Ortenzio, F., Dulac, F., Taillandier, V., Doglioli, A., Petrenko, A., Barrillon, S., Mallet, M., Nabat, P. and Desboeufs, K.: Process studies at the air-sea interface after atmospheric deposition in the Mediterranean Sea: objectives and strategy of the PEACETIME oceanographic campaign (May–June 2017), Biogeosciences Discussions, 2020, 1–65, doi:10.5194/bg-2020-44, 2020.

Herut, B., Zohary, T., Krom, M. D., Mantoura, R. F. C., Pitta, P., Psarra, S., Rassoulzadegan, F., Tanaka, T. and Frede Thingstad, T.: Response of East Mediterranean surface water to Saharan dust: On-board microcosm experiment and field observations, Deep Sea Research Part II: Topical Studies in Oceanography, 52(22), 3024–3040, doi:10.1016/j.dsr2.2005.09.003, 2005.

Holmes, R. M., Aminot, A., Kérouel, R., Hooker, B. A. and Peterson, B. J.: A simple and precise

method for measuring ammonium in marine and freshwater ecosystems, Can. J. Fish. Aquat. Sci., 56(10), 1801–1808, doi:10.1139/f99-128, 1999.

IPCC: Climate Change, The Physical Science Basis., 2013.

IPCC: IPCC Special Report on the Ocean and Cryosphere in a Changing Climate, edited by H. O. Pörtner, D. C. Roberts, V. Masson-Delmotte, P. Zhai, M. Tignor, E. Poloczanska, K. Mintenbeck, A. Alegría, M. Nicolai, A. Okem, J. Petzold, B. Rama, and N. M. Weyer., 2019.

Irwin, A. J. and Oliver, M. J.: Are ocean deserts getting larger?, Geophysical Research Letters, 36, doi:10.1029/2009gl039883, 2009.

Jickells, T. D., An, Z. S., Andersen, K. K., Baker, A. R., Bergametti, G., Brooks, N., Cao, J. J., Boyd, P. W., Duce, R. A., Hunter, K. A., Kawahata, H., Kubilay, N., laRoche, J., Liss, P. S., Mahowald, N., Prospero, J. M., Ridgwell, A. J., Tegen, I. and Torres, R.: Global Iron Connections Between Desert Dust, Ocean Biogeochemistry, and Climate, Science, 308(5718), 67–71, doi:10.1126/science.1105959, 2005.

Kana, T. M. and Glibert, P. M.: Effect of irradiances up to 2000 μE m^{-2} s^{-1} on marine *Synechococcus* WH7803—I. Growth, pigmentation, and cell composition, Deep Sea Research Part A. Oceanographic Research Papers, 34(4), 479–495, doi:10.1016/0198-0149(87)90001-X, 1987.

Kapsenberg, L., Alliouane, S., Gazeau, F., Mousseau, L. and Gattuso, J. P.: Coastal ocean acidification and increasing total alkalinity in the northwestern Mediterranean Sea, Ocean Science, 13(3), 411–426, doi:10.5194/os-13-411-2017, 2017.

1021 Kouvarakis, G., Mihalopoulos, N., Tselepides, A. and Stavrakakis, S.: On the importance of
1022 atmospheric inputs of inorganic nitrogen species on the productivity of the Eastern
1023 Mediterranean Sea, Global Biogeochemical Cycles, 15(4), 805–817,
1024 doi:10.1029/2001GB001399, 2001.

1025 Lagaria, A., Mandalakis, M., Mara, P., Papageorgiou, N., Pitta, P., Tsiola, A., Kagiorgi, M. and
1026 Psarra, S.: Phytoplankton response to Saharan dust depositions in the Eastern Mediterranean
1027 Sea: A mesocosm study, Front. Mar. Sci., 3, doi:10.3389/fmars.2016.00287, 2017.

1028 Law, C. S., Brévière, E., de Leeuw, G., Garçon, V., Guieu, C., Kieber, D. J., Kontradowitz, S.,
1029 Paulmier, A., Quinn, P. K., Saltzman, E. S., Stefels, J. and von Glasow, R.: Evolving
1030 research directions in Surface Ocean - Lower Atmosphere (SOLAS) science, Environ.
1031 Chem., 10(1), 1, doi:10.1071/EN12159, 2013.

1032 Lee, S. and Fuhrman, J. A.: Relationships between Biovolume and Biomass of Naturally Derived
1033 Marine Bacterioplankton, Appl Environ Microbiol, 53(6), 1298–1303, 1987.

1034 Lekunberri, I., Lefort, T., Romero, E., Vázquez-Domínguez, E., Romera-Castillo, C., Marrasé, C.,
1035 Peters, F., Weinbauer, M. and Gasol, J. M.: Effects of a dust deposition event on coastal
1036 marine microbial abundance and activity, bacterial community structure and ecosystem
1037 function, J Plankton Res, 32(4), 381–396, doi:10.1093/plankt/fbp137, 2010.

1038 Liu, X., Patsavas, M. C. and Byrne, R. H.: Purification and Characterization of meta-Cresol Purple
1039 for Spectrophotometric Seawater pH Measurements, Environ. Sci. Technol., 45(11),
1040 4862–4868, doi:10.1021/es200665d, 2011.

1041 Longhurst, A., Sathyendranath, S., Platt, T. and Caverhill, C.: An estimate of global primary
1042 production in the ocean from satellite radiometer data, Journal of Plankton Research, 17(6),

1245–1271, doi:10.1093/plankt/17.6.1245, 1995.

López-Urrutia, A. and Morán, X. A. G.: Resource limitation of bacterial production distorts the temperature dependence of oceanic carbon cycling, Ecology, 88(4), 817–822, doi:10.1890/06-1641, 2007.

Louis, J., Pedrotti, M. L., Gazeau, F. and Guieu, C.: Experimental evidence of formation of transparent exopolymer particles (TEP) and POC export provoked by dust addition under current and high pCO2 conditions, PLOS ONE, 12(2), e0171980, doi:10.1371/journal.pone.0171980, 2017a.

Louis, J., Guieu, C. and Gazeau, F.: Nutrient dynamics under different ocean acidification scenarios in a low nutrient low chlorophyll system: The Northwestern Mediterranean Sea, Estuarine, Coastal and Shelf Science, 186, 30–44, doi:10.1016/j.ecss.2016.01.015, 2017b.

Louis, J., Gazeau, F. and Guieu, C.: Atmospheric nutrients in seawater under current and high pCO_2 conditions after Saharan dust deposition: Results from three minicosm experiments, Progress in Oceanography, 163, 40–49, doi:10.1016/j.pocean.2017.10.011, 2018.

Loÿe-Pilot, M. D. and Martin, J. M.: Saharan Dust Input to the Western Mediterranean: An Eleven Years Record in Corsica, in The Impact of Desert Dust Across the Mediterranean, edited by S. Guerzoni and R. Chester, pp. 191–199, Springer Netherlands, Dordrecht., 1996.

Manca, B., Burca, M., Giorgetti, A., Coatanoan, C., Garcia, M.-J. and Iona, A.: Physical and biochemical averaged vertical profiles in the Mediterranean regions: an important tool to trace the climatology of water masses and to validate incoming data from operational oceanography, Journal of Marine Systems, 48(1), 83–116,

doi:10.1016/j.jmarsys.2003.11.025, 2004.

Marañón, E., Fernández, A., Mouriño-Carballido, B., MartÍnez-GarcÍa, S., Teira, E., Cermeño, P., Chouciño, P., Huete-Ortega, M., Fernández, E., Calvo-DÍaz, A., Morán, X. A. G., Bode, A., Moreno-Ostos, E., Varela, M. M., Patey, M. D. and Achterberg, E. P.: Degree of oligotrophy controls the response of microbial plankton to Saharan dust, Limnology and Oceanography, 55(6), 2339–2352, doi:10.4319/lo.2010.55.6.2339, 2010.

Marañón, E., Lorenzo, M. P., Cermeño, P. and Mouriño-Carballido, B.: Nutrient limitation suppresses the temperature dependence of phytoplankton metabolic rates, The ISME Journal, 12(7), 1836–1845, doi:10.1038/s41396-018-0105-1, 2018.

Marie, D., Simon, N., Guillou, L., Partensky, F. and Vaulot, D.: Flow cytometry analysis of marine picoplankton, in living color: protocols in flow cytometry and cell sorting, edited by R. A. Diamond and S. DeMaggio, pp. 421–454, Springer, Berlin., 2010.

Markaki, Z., Oikonomou, K., Kocak, M., Kouvarakis, G., Chaniotaki, A., Kubilay, N. and Mihalopoulos, N.: Atmospheric deposition of inorganic phosphorus in the Levantine Basin, eastern Mediterranean: Spatial and temporal variability and its role in seawater productivity, Limnology and Oceanography, 48(4), 1557–1568, doi:10.4319/lo.2003.48.4.1557, 2003.

Maugendre, L., Gattuso, J.-P., Louis, J., de Kluijver, A., Marro, S., Soetaert, K. and Gazeau, F.: Effect of ocean warming and acidification on a plankton community in the NW Mediterranean Sea, ICES Journal of Marine Science: Journal du Conseil, 72(6), 1744–1755, doi:10.1093/icesjms/fsu161, 2015.

Maugendre, L., Guieu, C., Gattuso, J.-P. and Gazeau, F.: Ocean acidification in the Mediterranean Sea: Pelagic mesocosm experiments. A synthesis, Estuarine, Coastal and Shelf Science, 186,

1086 1–10, doi:10.1016/j.ecss.2017.01.006, 2017.

1087 Mayot, N., D'Ortenzio, F., Ribera d'Alcalà, M., Lavigne, H. and Claustre, H.: Interannual
1088 variability of the Mediterranean trophic regimes from ocean color satellites, Biogeosciences,
1089 13(6), 1901–1917, doi:https://doi.org/10.5194/bg-13-1901-2016, 2016.

1090 Moore, C. M., Mills, M. M., Arrigo, K. R., Berman-Frank, I., Bopp, L., Boyd, P. W., Galbraith, E.
1091 D., Geider, R. J., Guieu, C., Jaccard, S. L., Jickells, T. D., La Roche, J., Lenton, T. M.,
1092 Mahowald, N. M., Marañón, E., Marinov, I., Moore, J. K., Nakatsuka, T., Oschlies, A.,
1093 Saito, M. A., Thingstad, T. F., Tsuda, A. and Ulloa, O.: Processes and patterns of oceanic
1094 nutrient limitation, Nature Geoscience, 6(9), 701–710, doi:10.1038/ngeo1765, 2013.

1095 Morán, X. A. G., López‐Urrutia, Á., Calvo‐Díaz, A. and Li, W. K. W.: Increasing importance of
1096 small phytoplankton in a warmer ocean, Global Change Biology, 16(3), 1137–1144,
1097 doi:10.1111/j.1365-2486.2009.01960.x, 2010.

1098 Neale, P. J., Sobrino, C., Segovia, M., Mercado, J. M., Leon, P., Cortés, M. D., Tuite, P., Picazo, A.,
1099 Salles, S., Cabrerizo, M. J., Prasil, O., Montecino, V., Reul, A. and Fuentes-Lema, A.: Effect
1100 of CO2, nutrients and light on coastal plankton. I. Abiotic conditions and biological
1101 responses, Aquatic Biology, 22, 25–41, doi:10.3354/ab00587, 2014.

1102 Orr, J. C., Epitalon, J.-M., Dickson, A. G. and Gattuso, J.-P.: Routine uncertainty propagation for
1103 the marine carbon dioxide system, Marine Chemistry, 207, 84–107,
1104 doi:10.1016/j.marchem.2018.10.006, 2018.

1105 Paytan, A., Mackey, K. R. M., Chen, Y., Lima, I. D., Doney, S. C., Mahowald, N., Labiosa, R. and
1106 Post, A. F.: Toxicity of atmospheric aerosols on marine phytoplankton, Proceedings of the

National Academy of Sciences, 106(12), 4601–4605, doi:10.1073/pnas.0811486106, 2009.

Pitta, P., Kanakidou, M., Mihalopoulos, N., Christodoulaki, S., Dimitriou, P. D., Frangoulis, C., Giannakourou, A., Kagiorgi, M., Lagaria, A., Nikolaou, P., Papageorgiou, N., Psarra, S., Santi, I., Tsapakis, M., Tsiola, A., Violaki, K. and Petihakis, G.: Saharan Dust Deposition Effects on the Microbial Food Web in the Eastern Mediterranean: A Study Based on a Mesocosm Experiment, Front. Mar. Sci., 4, doi:10.3389/fmars.2017.00117, 2017.

Polovina, J. J., Howell, E. A. and Abecassis, M.: Ocean's least productive waters are expanding, Geophysical Research Letters, 35(3), doi:10.1029/2007gl031745, 2008.

Pulido-Villena, E., Wagener, T. and Guieu, C.: Bacterial response to dust pulses in the western Mediterranean: Implications for carbon cycling in the oligotrophic ocean, Global Biogeochemical Cycles, 22(1), doi:10.1029/2007gb003091, 2008.

Pulido-Villena, E., Rérolle, V. and Guieu, C.: Transient fertilizing effect of dust in P-deficient LNLC surface ocean, Geophysical Research Letters, 37(1), doi:10.1029/2009GL041415, 2010.

Pulido-Villena, E., Baudoux, A.-C., Obernosterer, I., Landa, M., Caparros, J., Catala, P., Georges, C., Harmand, J. and Guieu, C.: Microbial food web dynamics in response to a Saharan dust event: results from a mesocosm study in the oligotrophic Mediterranean Sea, Biogeosciences, 11(19), 5607–5619, 2014.

Putaud, J.-P., Dingenen, R. V., Dell'Acqua, A., Raes, F., Matta, E., Decesari, S., Facchini, M. C. and Fuzzi, S.: Size-segregated aerosol mass closure and chemical composition in Monte Cimone (I) during MINATROC, Atmospheric Chemistry and Physics, 4(4), 889–902,

doi:https://doi.org/10.5194/acp-4-889-2004, 2004.

Ras, J., Claustre, H. and Uitz, J.: Spatial variability of phytoplankton pigment distributions in the Subtropical South Pacific Ocean: comparison between in situ and predicted data, Biogeosciences, 5(2), 353–369, doi:10.5194/bg-5-353-2008, 2008.

Regaudie-de-Gioux, A., Vaquer-Sunyer, R. and Duarte, C. M.: Patterns in planktonic metabolism in the Mediterranean Sea, Biogeosciences, 6(12), 3081–3089, doi:https://doi.org/10.5194/bg-6-3081-2009, 2009.

Richon, C., Dutay, J.-C., Dulac, F., Wang, R., Balkanski, Y., Nabat, P., Aumont, O., Desboeufs, K., Laurent, B., Guieu, C., Raimbault, P. and Beuvier, J.: Modeling the impacts of atmospheric deposition of nitrogen and desert dust-derived phosphorus on nutrients and biological budgets of the Mediterranean Sea, Progress in Oceanography, 163, 21–39, doi:10.1016/j.pocean.2017.04.009, 2018.

Ridame, C. and Guieu, C.: Saharan input of phosphate to the oligotrophic water of the open western Mediterranean Sea, Limnology and Oceanography, 47(3), 856–869, 2002.

Ridame, C., Bigeard, E., Dinasquet, J., Tovar-Sanchez, A., Baudoux, A.-C., Gazeau, F. and Guieu, C.: Impact of dust enrichment on N_2 fixation and diversity of diazotrophs under present and future conditions of pH and temperature, Biogeosciences, in preparation.

Ridame, C., Dekaezemacker, J., Guieu, C., Bonnet, S., L'Helguen, S. and Malien, F.: Contrasted Saharan dust events in LNLC environments: impact on nutrient dynamics and primary production, Biogeosciences (BG), 11(17), 4783–4800, 2014.

Romero, E., Peters, F., Marrasé, C., Guadayol, Ò., Gasol, J. M. and Weinbauer, M. G.: Coastal

1149 Mediterranean plankton stimulation dynamics through a dust storm event: An experimental
1150 simulation, Estuarine, Coastal and Shelf Science, 93(1), 27–39,
1151 doi:10.1016/j.ecss.2011.03.019, 2011.

1152 Roy-Barman, M., Foliot, L., Douville, E., Guieu, C., Leblond, N., Gazeau, F., Bressac, M.,
1153 Wagener, T. and Ridame, C.: Contrasted release of insoluble elements (Fe, Al, REE, Th, Pa)
1154 during dust deposition in seawater: a minicosm approach, Biogeosciences, in preparation.

1155 Sala, M. M., Aparicio, F. L., Balagué, V., Boras, J. A., Borrull, E., Cardelús, C., Cros, L., Gomes,
1156 A., López-Sanz, A., Malits, A., Martínez, R. A., Mestre, M., Movilla, J., Sarmento, H.,
1157 Vázquez-Domínguez, E., Vaqué, D., Pinhassi, J., Calbet, A., Calvo, E., Gasol, J. M.,
1158 Pelejero, C. and Marrasé, C.: Contrasting effects of ocean acidification on the microbial
1159 food web under different trophic conditions, ICES Journal of Marine Science, 73(3),
1160 670–679, doi:10.1093/icesjms/fsv130, 2016.

1161 Sherr, E. B. and Sherr, B. F.: Bacterivory and herbivory: Key roles of phagotrophic protists in
1162 pelagic food webs, Microb Ecol, 28(2), 223–235, doi:10.1007/BF00166812, 1994.

1163 Siokou-Frangou, I., Christaki, U., Mazzocchi, M. G., Montresor, M., Ribera d'Alcalá, M., Vaqué,
1164 D. and Zingone, A.: Plankton in the open Mediterranean Sea: a review, Biogeosciences,
1165 7(5), 1543–1586, doi:https://doi.org/10.5194/bg-7-1543-2010, 2010.

1166 Tanaka, T., Thingstad, T. F., Christaki, U., Colombet, J., Cornet-Barthaux, V., Courties, C.,
1167 Grattepanche, J.-D., Lagaria, A., Nedoma, J., Oriol, L., Psarra, S., Pujo-Pay, M. and
1168 Wambeke, F. V.: Lack of P-limitation of phytoplankton and heterotrophic prokaryotes in
1169 surface waters of three anticyclonic eddies in the stratified Mediterranean Sea,
1170 Biogeosciences, 8(2), 525–538, doi:https://doi.org/10.5194/bg-8-525-2011, 2011.

Ternon, E., Guieu, C., Loÿe-Pilot, M.-D., Leblond, N., Bosc, E., Gasser, B., Miquel, J.-C. and Martín, J.: The impact of Saharan dust on the particulate export in the water column of the North Western Mediterranean Sea, Biogeosciences, 7(3), 809–826, doi:https://doi.org/10.5194/bg-7-809-2010, 2010.

The Mermex group: Marine ecosystems' responses to climatic and anthropogenic forcings in the Mediterranean, Progress in Oceanography, 91(2), 97–166, doi:10.1016/j.pocean.2011.02.003, 2011.

Theodosi, C., Markaki, Z., Tselepides, A. and Mihalopoulos, N.: The significance of atmospheric inputs of soluble and particulate major and trace metals to the eastern Mediterranean seawater, Marine Chemistry, 120(1), 154–163, doi:10.1016/j.marchem.2010.02.003, 2010.

Verity, P. G., Robertson, C. Y., Tronzo, C. R., Andrews, M. G., Nelson, J. R. and Sieracki, M. E.: Relationships between cell volume and the carbon and nitrogen content of marine photosynthetic nanoplankton, Limnology and Oceanography, 37(7), 1434–1446, doi:10.4319/lo.1992.37.7.1434, 1992.

Vidussi, F., Claustre, H., Manca, B. B., Luchetta, A. and Marty, J.-C.: Phytoplankton pigment distribution in relation to upper thermocline circulation in the eastern Mediterranean Sea during winter, Journal of Geophysical Research: Oceans, 106(C9), 19939–19956, doi:10.1029/1999JC000308, 2001.

Tables

Table 1. List of investigated parameters and processes during the three experiments at stations TYR, ION and FAST. Related manuscripts are indicated. pH_T: pH on the total scale, A_T: total alkalinity, ^{13}C-C_T: ^{13}C signature of dissolved inorganic carbon, NO_x: nitrate + nitrite, DIP: dissolved inorganic phosphorus, $Si(OH)_4$: silicate, DFe: dissolved iron, DAl: dissolved aluminium, Th-REE-Pa: Thorium (230Th and 232Th), Rare Earth elements and Protactinium (231Pa), POC: particulate organic carbon, DOC: dissolved organic carbon, ^{13}C-DOC: ^{13}C signature of dissolved organic carbon, TEP: transparent exopolymeric particles, NCP/CR: net community production and community respiration (oxygen based), ^{14}C-PP: primary production based on ^{14}C incorporation.

Sampling time	T-1	T0	T1	T2	T3	T4	T5	T6 / T7	Related manuscript
	Filling tanks	Before seeding, after warming / acidification)	+1 h	+6 h	+12 h	+24 h	+48 h	+72 h/+96 h	
Temperature	Continuous								This manuscript
Irradiance	Continuous								This manuscript
Carbonate chemistry									
pH_T									This manuscript
A_T									This manuscript
$\delta^{13}C$-C_T									Gazeau et al. (in preparation)
Macro-nutrients									
NO_x									This manuscript
DIP									This manuscript
$Si(OH)_4$									This manuscript
Micro-nutrients									
DFe									Roy-Barman et al. (in preparation)

DAl	Roy-Barman et al. (in preparation)
Th-REE-Pa	Roy-Barman et al. (in preparation)
Biological stocks	
Pigments	This manuscript
Flow cytometry	This manuscript
Microscopy	This manuscript
Diazotroph abundance	Ridame et al. (in preparation)
Virus abundance	Dinasquet et al. (in preparation)
Meta-transcriptomics	Dinasquet et al. (in preparation)
Bacterial diversity	Dinasquet et al. (in preparation)
Micro-eukaryote diversity	Dinasquet et al. (in preparation)
Meso-zooplankton	This manuscript
POC (incl. $\delta^{13}C$)	Gazeau et al. (in preparation)
POC sediment traps	Gazeau et al. (in preparation)
DOC	Gazeau et al. (in preparation)
^{13}C-DOC	Gazeau et al. (in preparation)
TEP	Gazeau et al. (in preparation)

	Amino acids	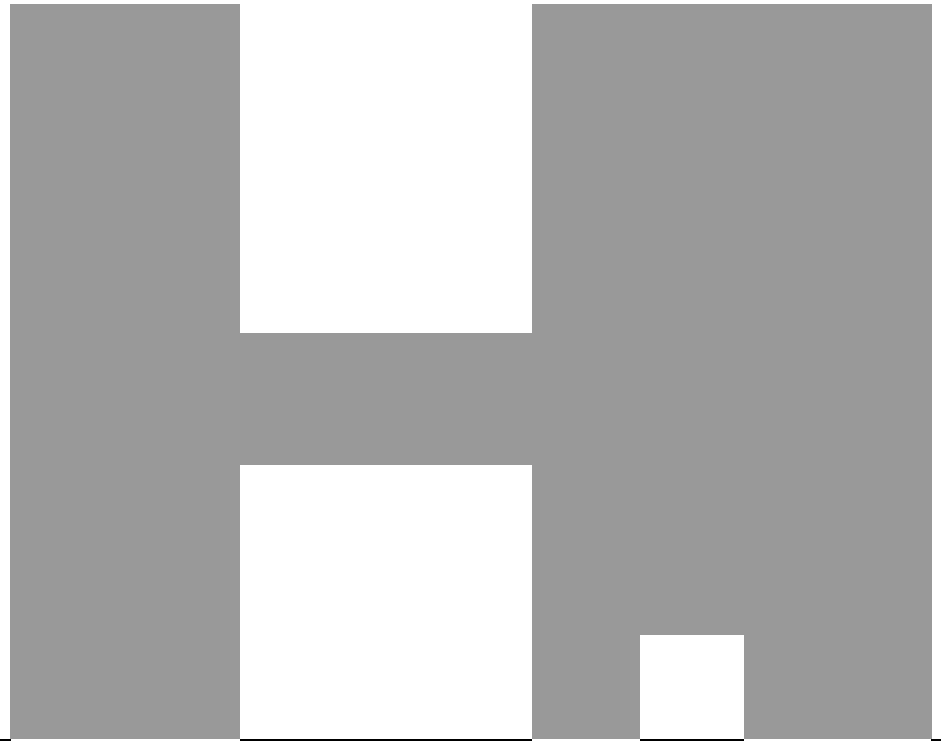	Gazeau et al. (in preparation)
	Carbohydrates		Gazeau et al. (in preparation)
Processes			
	NCP/CR		Gazeau et al. (in preparation)
	^{14}C-PP		Gazeau et al. (in preparation)
	Heterotrophic production		Gazeau et al. (in preparation)
	Ectoenzymatic activity		Gazeau et al. (in preparation)
	N_2 fixation		Ridame et al. (in preparation)
	$^{13}CO_2$-fixation		Ridame et al. (in preparation) Gazeau et al. (in preparation)
	Virus production, lysogeny		Dinasquet et al. (in preparation)

Table 2. Initial conditions as measured while filling the tanks (initial conditions in pumped surface water; sampling time: t-12h). pH_T: pH on the total scale, NO_x: nitrate + nitrite, NH_4: ammonium, DIP: dissolved inorganic phosphorus, $Si(OH)_4$: silicate, TChl*a*: total chlorophyll *a*, HNF: heterotrophic nanoflagellates. The three most important pigments in terms of concentration are also presented (19'-hexanoyloxyfucoxanthin, Zeaxanthin and Divinyl Chlorophyll *a*). Biomasses of the different groups analyzed through flow cytometry were estimated based on conversion equations and/or factors found in the literature (see section 2.3). Autotrophic biomass was, as a first approximation, estimated only based on flow cytometry data and therefore corresponds to the fraction < 20 µm. Heterotrophic biomass was estimated as the sum of heterotrophic prokaryote and HNF biomasses (see section 2.3). Values below detection limits are indicated as < dl.

	Sampling station	TYR	ION	FAST
	Coordinates (decimal)	39.34 N, 12.60 E	35.49 N, 19.78 E	37.95 N, 2.90 N
	Bottom depth (m)	3395	3054	2775
	Day and time of sampling (local time)	17/05/2017 17:00	25/05/2017 17:00	02/06/2017 21:00
	Temperature (°C)	20.6	21.2	21.5
	Salinity	37.96	39.02	37.07
Carbonate chemistry	pH_T	8.04	8.07	8.03
	Total alkalinity (μmol kg^{-1})	2529	2627	2443
Nutrients	NO_x (nmol L^{-1})	14.0	18.0	59.0
	NH_4^+ (μmol L^{-1})	0.045	0.022	< dl
	DIP (nmol L^{-1})	17.1	6.5	12.9
	$Si(OH)_4$ (μmol L^{-1})	1.0	0.96	0.64
	NO_x/DIP (molar ratio)	0.8	2.5	4.6
Pigments	TChl*a* (μg L^{-1})	0.063	0.066	0.072
	19'-hexanoyloxyfucoxanthin (μg L^{-1})	0.017	0.021	0.016
	Zeaxanthin (μg L^{-1})	0.009	0.006	0.036
	Divinyl Chlorophyll *a* (μg L^{-1})	~ 0	0	0.014

Flow cytometry	Pico-eukaryotes (abundance in cell mL^{-1}; biomass in µg C L^{-1})	347.8; 0.5	239.9; 0.4	701.0; 1.0
	Nano-eukaryotes (abundance in cell mL^{-1}; biomass in µg C L^{-1})	150.5; 3.9	188.8; 4.8	196.6; 5.0
	Synechococcus (abundance in cell mL^{-1}; biomass in µg C L^{-1})	4972; 1.2	3037; 0.8	6406; 1.6
	Autotrophic biomass (µg C L^{-1})	5.6	6.0	7.7
	Heterotrophic prokaryotes abundance (x 10^5 cell mL^{-1})	4.79	2.14	6.15
	HNF (abundance in cell mL^{-1})	110.1	53.6	126.2
	Heterotrophic biomass (µg C L^{-1})	9.9	4.5	12.7
Microscopy	Pennate diatoms (abundance in cell L^{-1})	140	520	880
	Centric diatoms (abundance in cell L^{-1})	200	380	580
	Dinoflagellates (abundance in cell L^{-1})	2770	3000	3410
	Autotrophic flagellates (abundance in cell L^{-1})	0	60	650
	Ciliates (abundance in cell L^{-1})	270	380	770

1212 Table 3. Maximum input of nitrate + nitrite (NO_x) and dissolved inorganic phosphorus (DIP)
1213 released from Saharan dust in tanks D and G as observed from the two discrete samplings
1214 performed over the first 6 h after seeding. The estimated maximal percentage of dissolution is also
1215 presented (see section 2.3 for details on the calculations).

	NO_x				DIP			
	D1	D2	G1	G2	D1	D2	G1	G2
Maximum input	μmol L^{-1}				nmol L^{-1}			
TYR	11.0	11.1	11.1	11.0	24.6	20.4	24.6	23.9
ION	11.2	11.6	11.2	11.3	23.3	22.0	19.6	22.9
FAST	11.3	11.1	11.1	11.2	30.8	31.3	36.9	29.8
Percentage of dissolution (%)								
TYR	95	96	95	94	12	10	12	11
ION	96	99	96	97	11	10	9	11
FAST	97	97	95	97	15	15	17	14

1216

Table 4. Removal rate of nitrate + nitrite (NO_x) and dissolved inorganic phosphorus (DIP) in tanks D and G during the three experiments (TYR, ION and FAST). For NO_x, decreasing rates were estimated based on linear regressions between maximal concentrations (i.e. after dust enrichment, at t1h or t6h) and final concentrations (t72 h for TYR and ION and t96h for FAST). For DIP, decreasing rates were estimated based on linear regressions between maximal concentrations (i.e. after dust enrichment at t1h or t6h) and concentrations measured at sampling times after which a stabilization was observed. This sampling time is shown in parentheses. All rates are expressed in nmol L^{-1} h^{-1}.

	NO_x			DIP		
	TYR	ION	FAST	TYR	ION	FAST
D1	-6.5	-8.6	-14.3	-0.4 (t72h)	-0.5 (t48h)	-0.2 (t96h)
D2	-1.0	-8.6	-13.5	-0.3 (t72h)	-0.8 (t24h)	-0.2 (t96h)
G1	-6.7	-13.1	-21.6	-1.3 (t24h)	-0.8 (t24h)	-1.5 (t24h)
G2	-0.8	-1.6	-25.2	-1.3 (t24h)	-1.6 (t24h)	-1.1 (t24h)

1226 Table 5. Maximum relative changes in tanks D and G as compared to controls (average between C1
1227 and C2), expressed as a %, for the three experiments (TYR, ION and FAST). The sampling time at
1228 which these maximum relative changes were observed is shown in brackets. Tchl*a* refers to the
1229 concentration of total chlorophyll *a* and B_{micro} to the biomass proxy of micro-phytoplankton (sum of
1230 Fucoxanthin and Peridinin, see Material and Methods) based on high performance liquid
1231 chromatography (HPLC). HP and HNF refer to heterotrophic prokaryote and heterotrophic
1232 nanoflagellate abundances, respectively, as measured by flow cytometry.

Experiment	Tank	HPLC		Flow cytometry				
		TChl*a*	B_{micro}	Pico-eukaryotes	Nano-eukaryotes	*Synechococcus*	HP	HNF
TYR	D1	-35 (t24h)	-33 (t12h)	-75 (t72h)	-80 (t1h)	-71 (t48h)	68 (t72h)	352 (t72h)
TYR	D2	-38 (t12h)	-39 (t24h)	-75 (t72h)	-80 (t1h)	-72 (t48h)	53 (t72h)	100 (t72h)
TYR	G1	60 (t72h)	52 (t72h)	-75 (t1h)	89 (t72h)	76 (t72h)	67 (t72h)	1095 (t72h)
TYR	G2	359 (t72h)	392 (t72h)	323 (t72h)	119 (t72h)	700 (t72h)	68 (t48h)	298 (t72h)
ION	D1	183 (t72h)	157 (t72h)	126 (t72h)	89 (t72h)	317 (t72h)	128 (t72h)	44 (t72h)
ION	D2	109 (t72h)	156 (t72h)	117 (t72h)	-59 (t1h)	390 (t72h)	133 (t72h)	27 (t72h)
ION	G1	399 (t72h)	454 (t72h)	458 (t72h)	256 (t72h)	805 (t72h)	176 (t72h)	175 (t72h)
ION	G2	426 (t72h)	612 (t72h)	510 (t72h)	292 (t72h)	1425 (t72h)	161 (t72h)	129 (t72h)
FAST	D1	318 (t96h)	356 (t96h)	113 (t96h)	208 (t72h)	348 (t96h)	27 (t96h)	-38 (t96h)
FAST	D2	237 (t96h)	322 (t96h)	91 (t96h)	219 (t72h)	197 (t96h)	40 (t48h)	-49 (t96h)
FAST	G1	399 (t96h)	415 (t96h)	198 (t72h)	274 (t72h)	357 (t48h)	61 (t48h)	243 (t24h)
FAST	G2	395 (t96h)	421 (t96h)	129 (t72h)	202 (t96h)	344 (t48h)	67 (t48h)	74 (t24h)

Figure captions

Fig. 1. Map showing the sampling stations in the Mediterranean Sea along the transect performed onboard the R/V “Pourquoi Pas ?” during the PEACETIME cruise.

Fig. 2. Scheme of an experimental tank (climate reactor).

Fig. 3. Proportion of the different pigments, as measured by high performance liquid chromatography (HPLC) in pumped surface seawater for the three experiments (t-12h).

Fig. 4. Continuous measurements of temperature and irradiance level (PAR) in the six tanks during the three experiments. The dashed vertical line indicates the time of dust seeding (after t0).

Fig. 5. pH on the total scale (pH_T) and total alkalinity (A_T) measured in the six tanks during the three experiments. The dashed vertical line indicates the time of dust seeding (after t0). Error bars correspond to the standard deviation based on analytical triplicates.

Fig. 6. Nutrients (nitrate + nitrite: NO_x, dissolved inorganic phosphorus: DIP, silicate: $Si(OH)_4$ as well as the molar ratio between NO_x and DIP, measured in the six tanks during the three experiments. The dashed vertical line indicates the time of seeding (after t0).

Fig. 7. Concentrations of total chlorophyll *a* and major pigments, measured by high performance liquid chromatography (HPLC), in the six tanks during the three experiments. The dashed vertical line indicates the time of seeding (after t0).

Fig. 8. Abundance of pico-eukaryotes, nano-eukaryotes, *Synechococcus,* heterotrophic prokaryotes (HP), and heterotrophic nano-flagellates (HNF), measured by flow cytometry, in the six tanks during the three experiments. The evolution of autotrophic biomass (see Material and Methods for

details on the calculation) is also shown. The dashed vertical line indicates the time of seeding (after t0).

Fig. 9. Abundances of meso-zooplankton species as measured at the end of each experiment.

Fig. 10. Maximal relative change (%) of main biological stocks (TCHl*a*: total chlorophyll *a*, HP: heterotrophic prokaryotes) and processes (BP: bacterial production; PP: ^{14}C-based primary production; see Gazeau et al., in preparation, this issue; BR: bacterial respiration (no data from this study); and N_2 fixation, see Ridame et al., in preparation, this issue) as obtained during the present study at the 3 stations (TYR, ION and FAST) under ambient conditions of pH and temperature (open red squares) and future conditions (full green squares). Squares are delimited by the range of responses observed among the duplicates for each treatment. The dotted green squares for station TYR denote the large variability observed between duplicates for some parameters and processes that prevented drawing solid conclusions. Box-plots represent the distribution of responses observed from studies conducted in the Mediterranean Sea, as compiled by Guieu and Ridame (2020).

1268

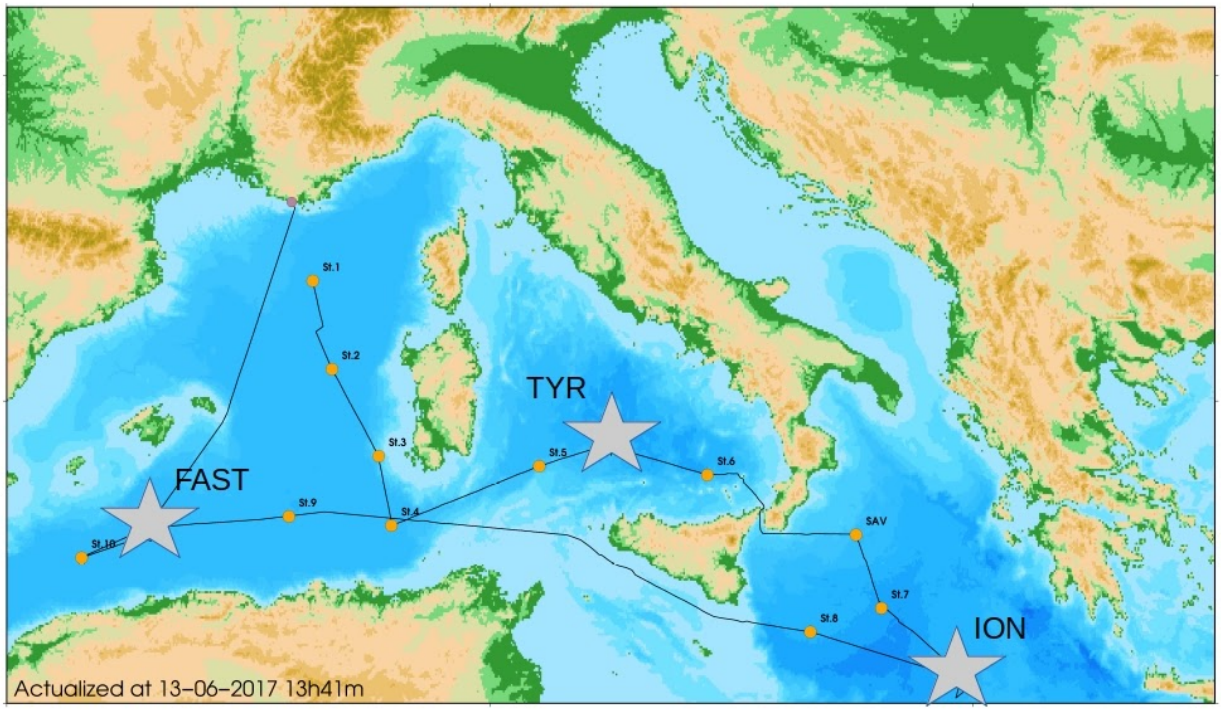

1269 Fig. 1.

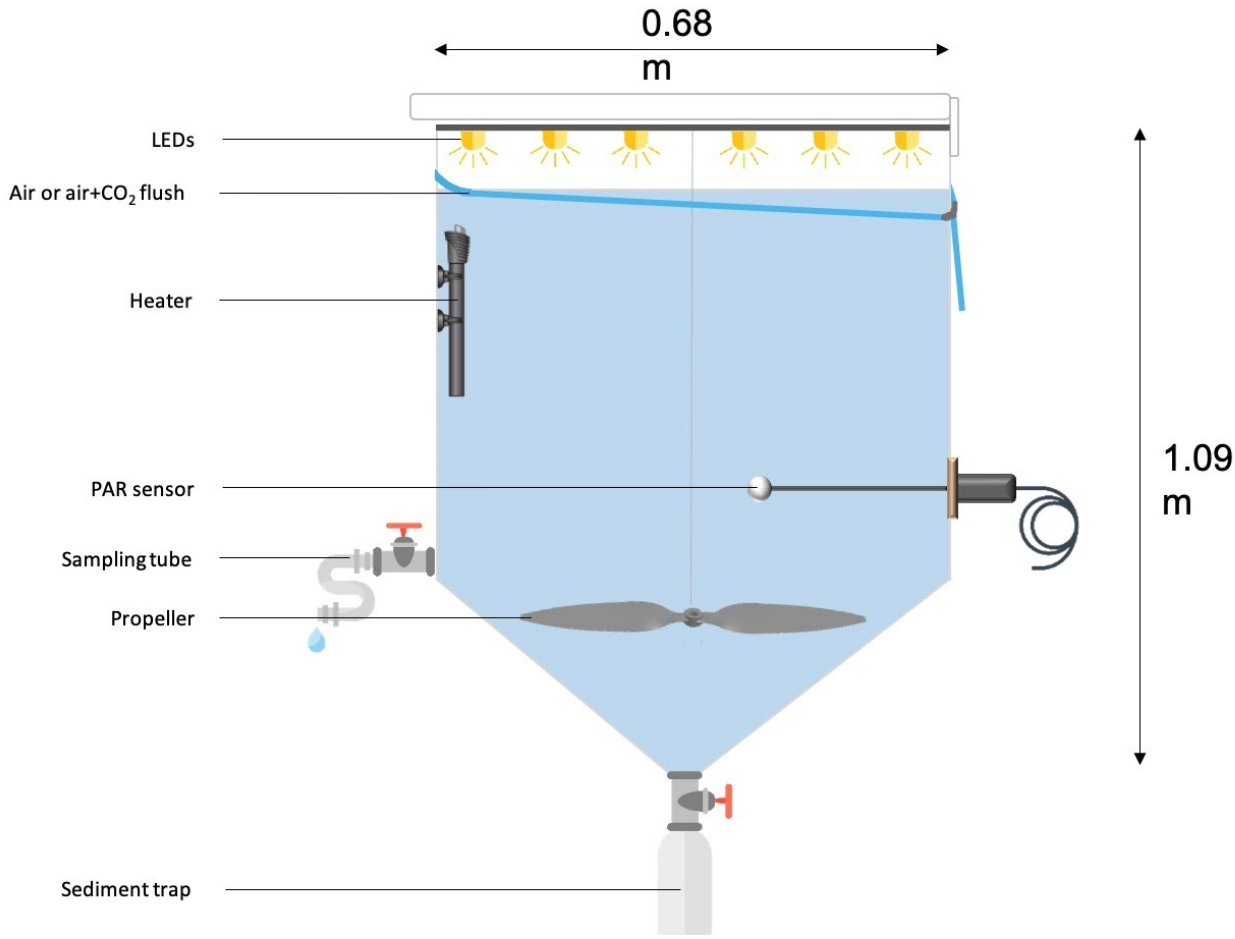
0.68
m
LEDs
Air or air+CO_2 flush
Heater
PAR sensor
Sampling tube
Propeller
Sediment trap
1.09
m

Fig. 2.

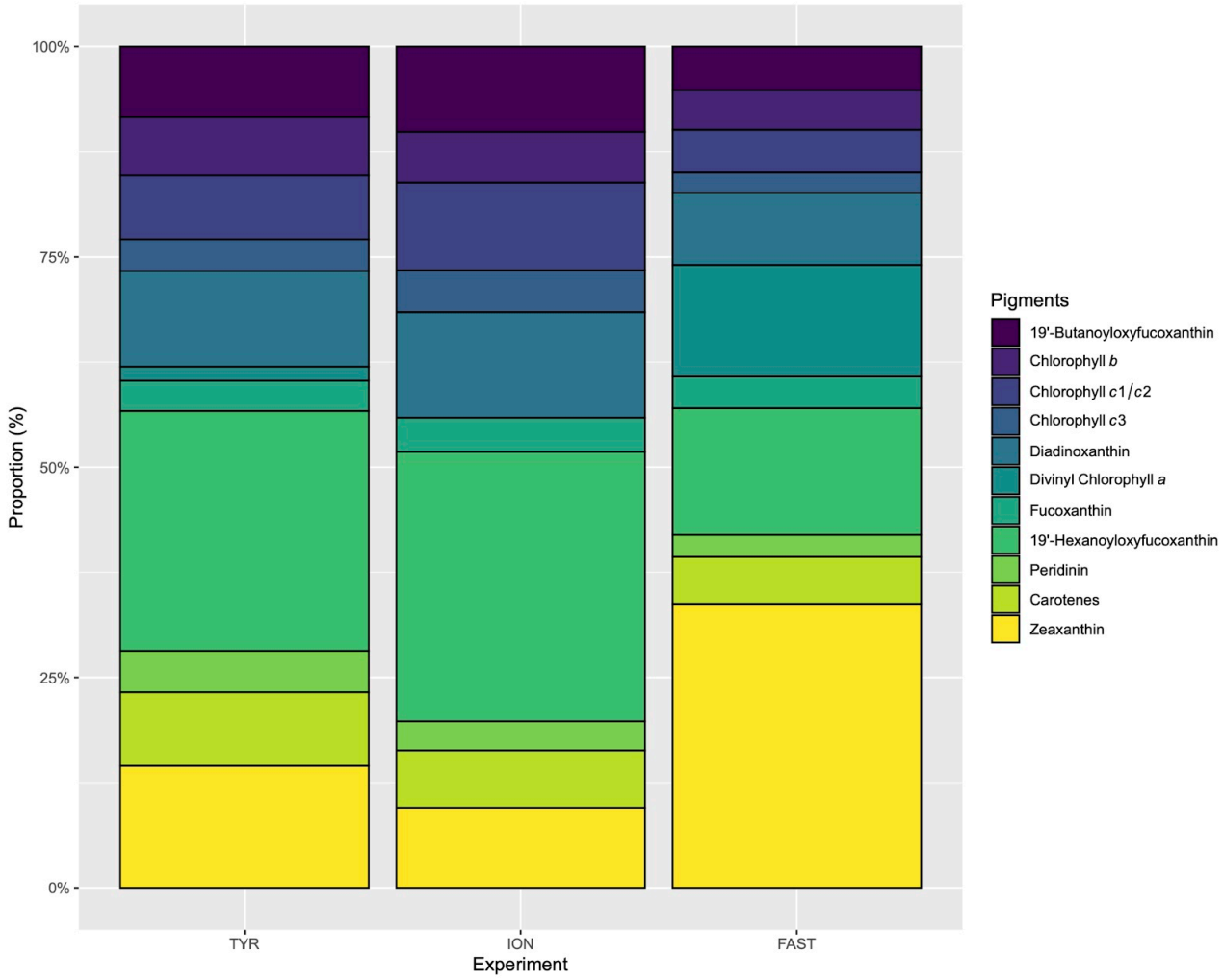

1272

1273 Fig. 3.

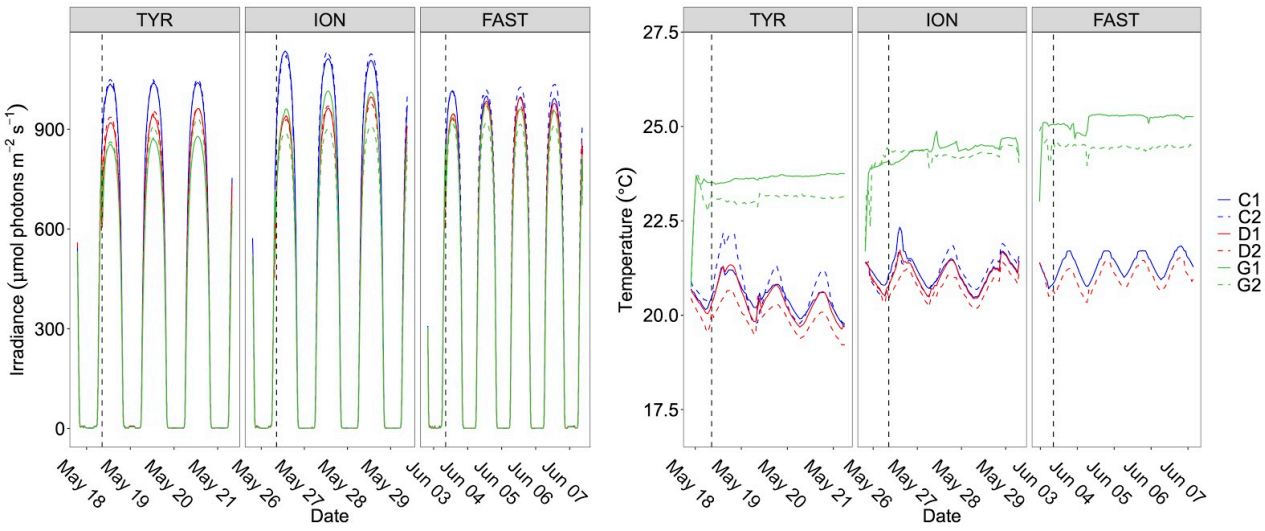
TYR
ION
FAST
Irradiance (µmol photons m^{-2} s^{-1})
0
300
600
900
Temperature (°C)
17.5
20.0
22.5
25.0
27.5
May 18
May 19
May 20
May 21
May 26
May 27
May 28
May 29
Jun 03
Jun 04
Jun 05
Jun 06
Jun 07
Date
C1
C2
D1
D2
G1
G2

Fig. 4.

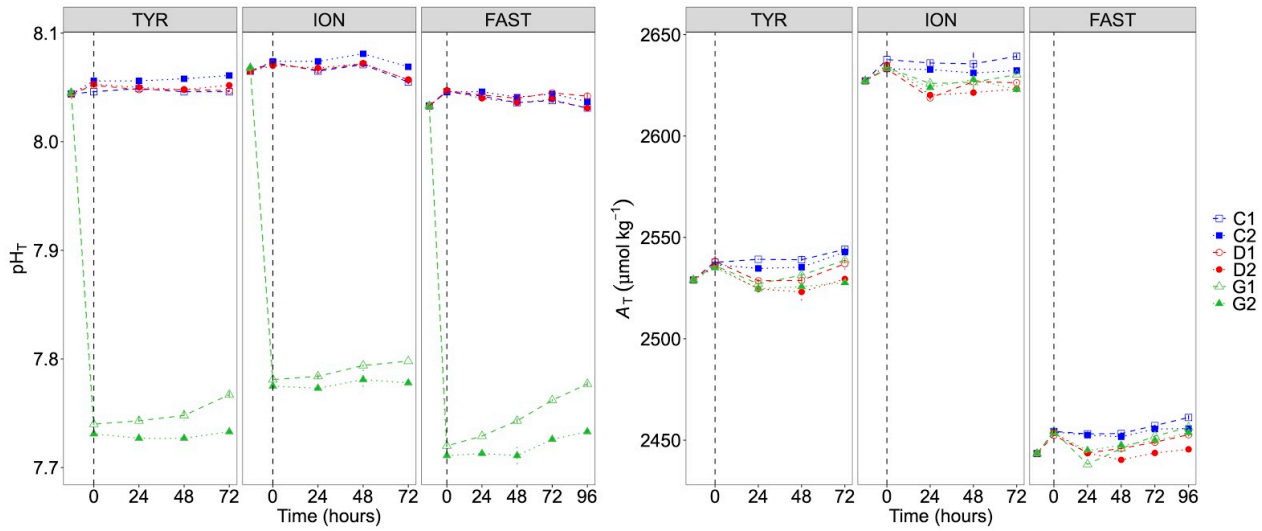
TYR
ION
FAST
8.1
8.0
7.9
7.8
7.7
pH$_T$
2650
2600
2550
2500
2450
A_T (µmol kg^{-1})
0
24
48
72
96
Time (hours)
C1
C2
D1
D2
G1
G2

Fig. 5.

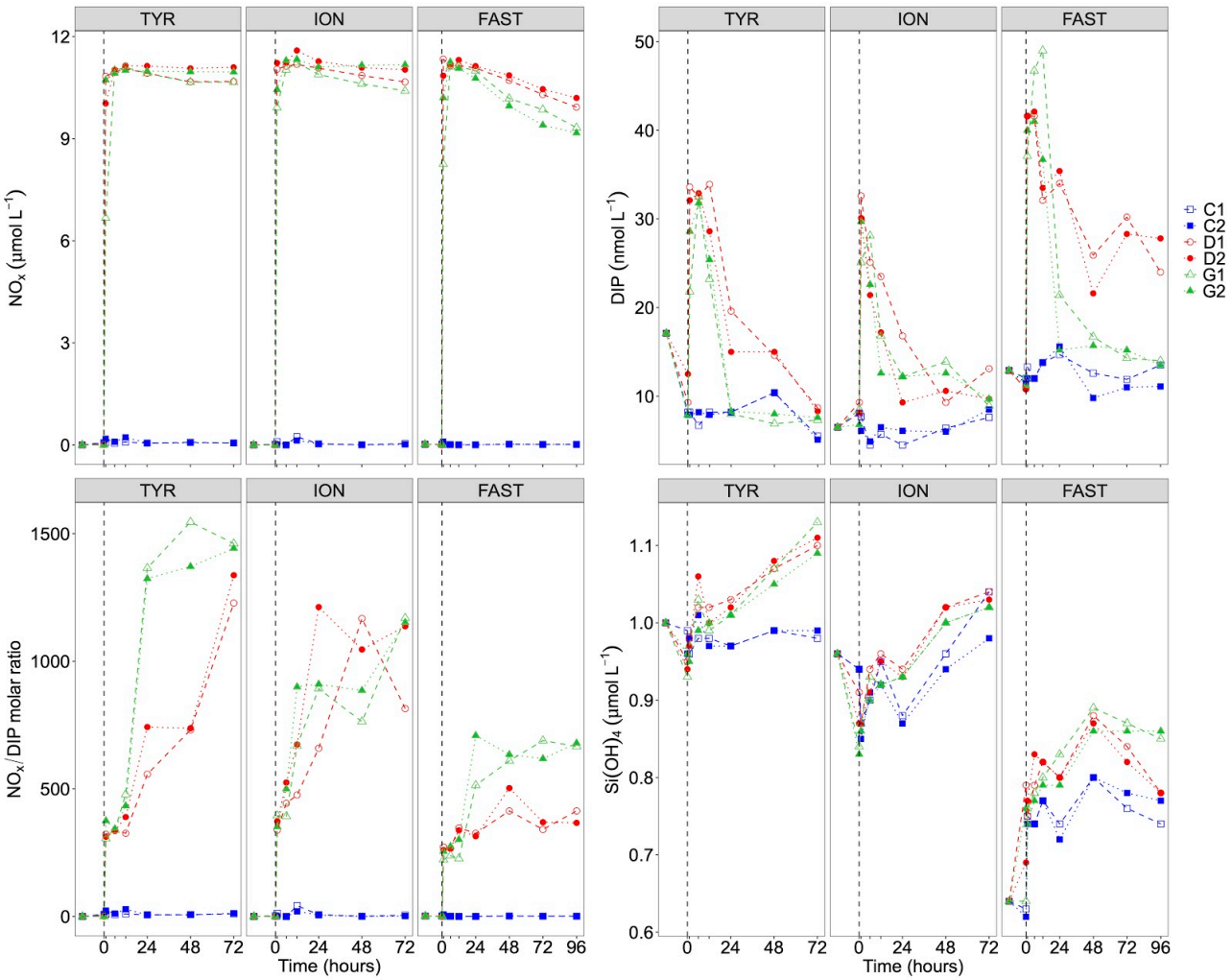

1278

1279 Fig. 6.

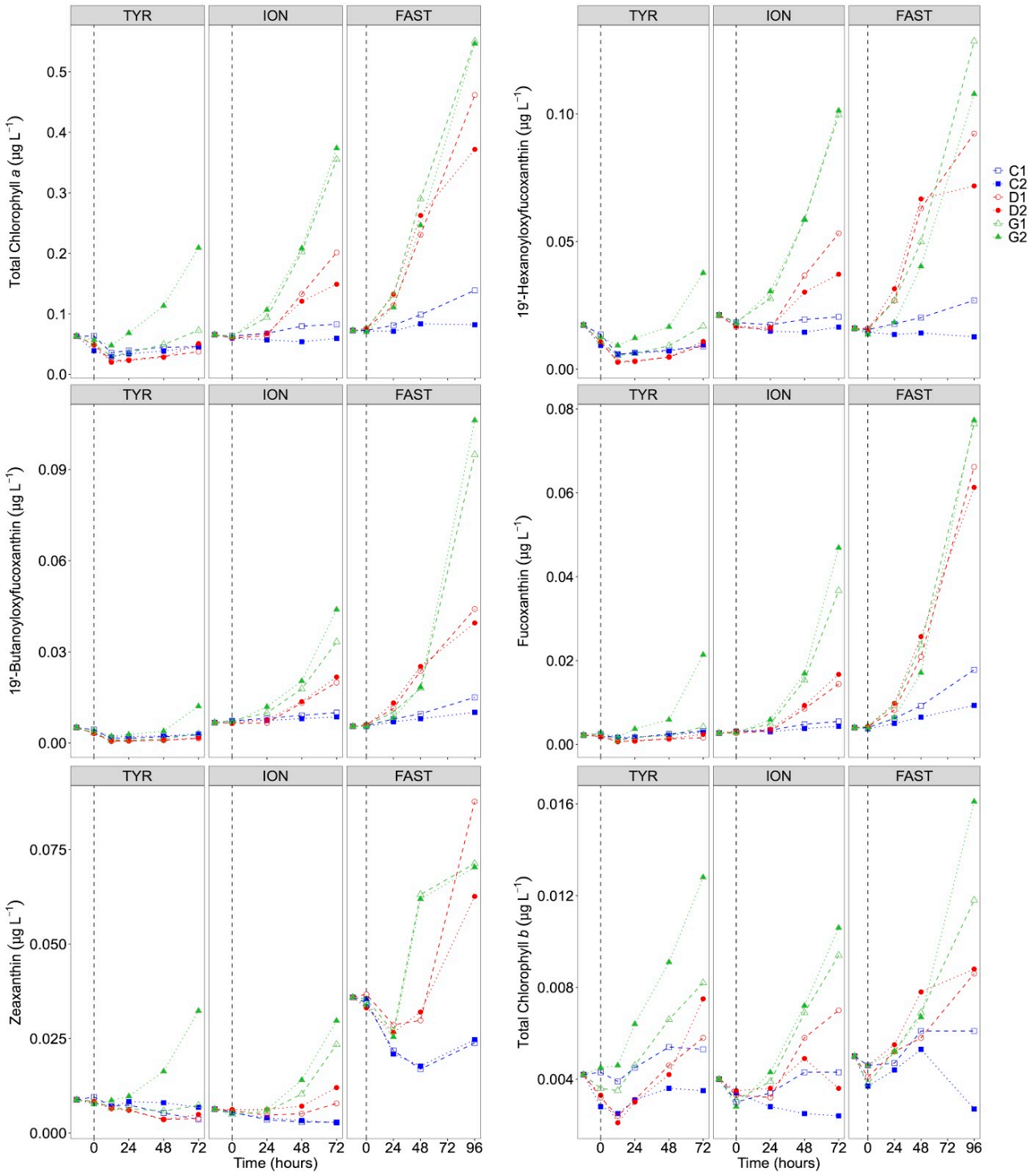

1280

1281 Fig. 7.

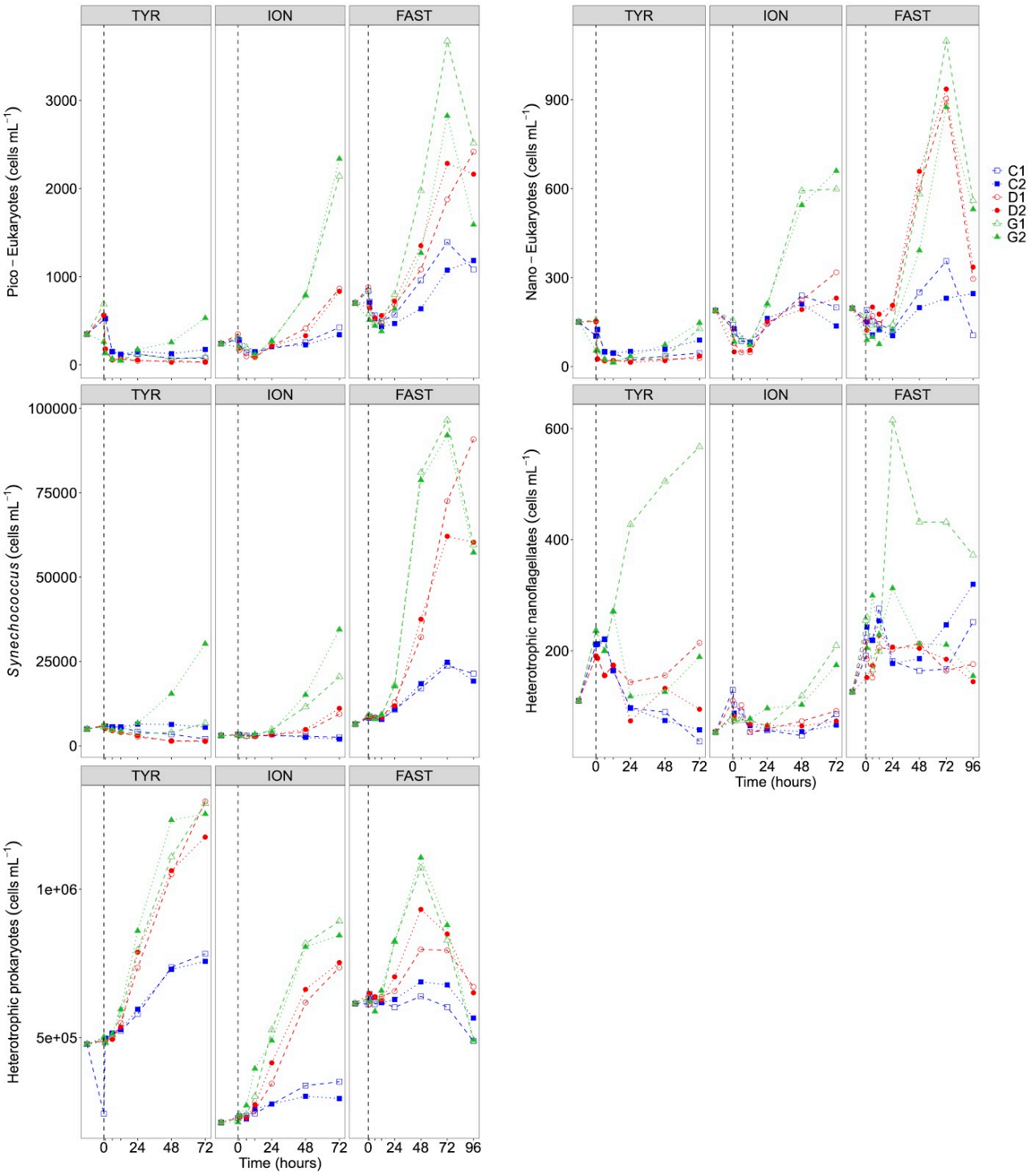

1282

1283 Fig. 8.

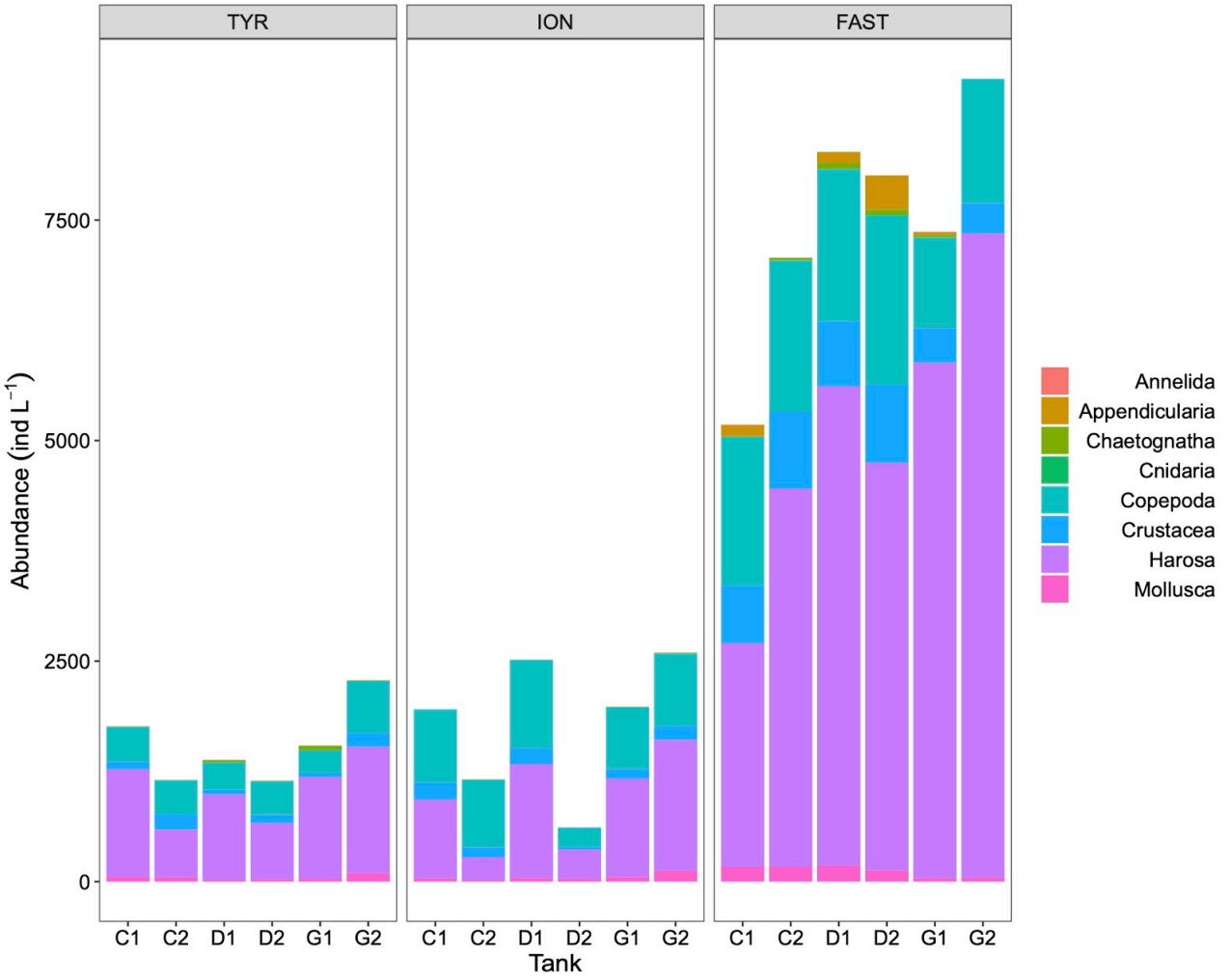
TYR
ION
FAST
Abundance (ind L^{-1})
7500
5000
2500
0
C1 C2 D1 D2 G1 G2
Tank
Annelida
Appendicularia
Chaetognatha
Cnidaria
Copepoda
Crustacea
Harosa
Mollusca

Fig. 9.

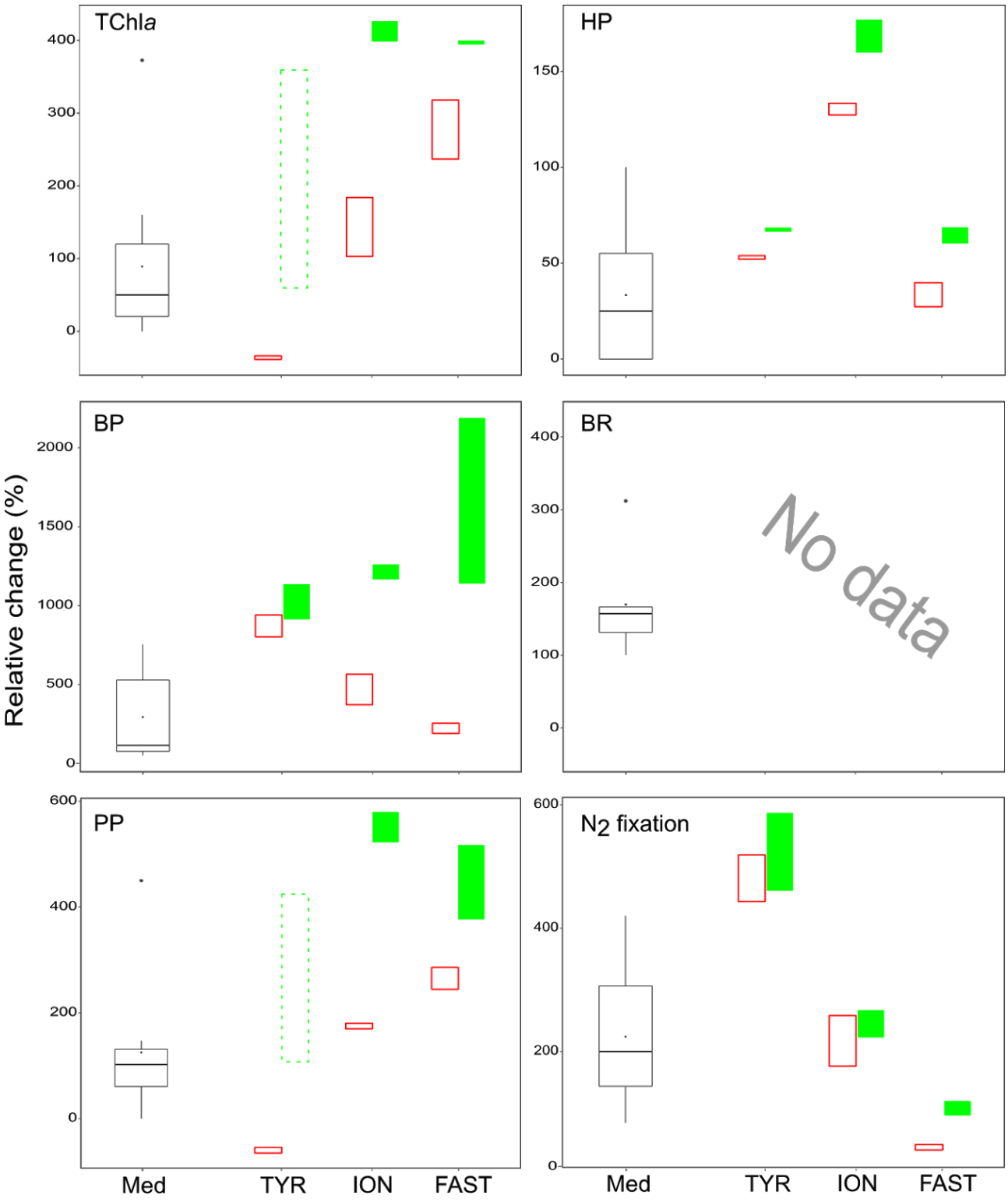

1286

1287 Fig. 10.